Acid-Base Catalysts for Polycondensation of Acetaldehyde in Flow

by

Marcella R. Lusardi

B.S. Chemical Engineering
Columbia University, 2012

M.S. Earth Resources Engineering
Columbia University, 2013

SUBMITTED TO THE DEPARTMENT OF MATERIALS SCIENCE AND ENGINEERING
IN PARTIAL FULFILLMENT OF THE REQUIREMENTS FOR THE DEGREE OF

MASTER OF SCIENCE IN MATERIALS SCIENCE AND ENGINEERING
AT THE
MASSACHUSETTS INSTITUTE OF TECHNOLOGY

SEPTEMBER 2015

Signature of Author: Signature redacted
Department of Materials Science and Engineering
July 31, 2015

Certified by: Signature redacted
Klavs F. Jensen
Warren K. Lewis Professor of Chemical Engineering and
Professor of Materials Science and Engineering
Thesis Supervisor

Accepted by: Signature redacted
Donald Sadoway
Chair, Departmental Committee on Graduate Students

Acid-Base Catalysts for Polycondensation of Acetaldehyde in Flow

by

Marcella R. Lusardi

Submitted to the Department of Materials Science and Engineering
on July 31, 2015 in Partial Fulfillment
of the Requirements for the Degree of Master of Science in
Materials Science and Engineering

ABSTRACT

Acetaldehyde is used as a bio-oil model compound in a polycondensation reaction over two acid-base catalysts, pelletized Evonik P25 TiO_2 and an activated hydrotalcite-like compound (HTlc), to produce high molecular weight molecules in the transportation fuel range. The catalytic performance of these materials is evaluated in a gas phase, atmospheric flow system with a packed bed microreactor designed to mimic process conditions in one step of the overall bio-oil upgrading scheme. The HTlc is activated through calcination at 500 °C followed by rehydration in decarbonated H_2O, generating the active acid-base hydroxyl pairs. Materials are characterized through XRD, low temperature N_2 adsorption-desorption isotherm experiments, TGA, and XPS. In initial experiments, high conversions are achieved but all converted acetaldehyde forms carbonaceous deposits on the catalyst surfaces over a range of temperatures and residence times. When the catalyst bed is reduced by 80%, decreasing both residence time and vapor-solid contact area, high conversions are maintained and the production of liquid phase condensation products is observed on the order of seconds. While yields are low, it is promising that tuning the packed bed results in decreased deposits and generation of liquid phase products. Further adjustments of reaction parameters and catalyst activity are of interest as future work, including shorter residence times and bed lengths, co-feeding a reaction inhibitor, and specific catalyst syntheses for control over active sites.

Thesis Supervisor: Klavs F. Jensen

Title: Warren K. Lewis Professor of Chemical Engineering and Professor of Materials Science and Engineering

Acknowledgements

I first thank my thesis advisor Klavs Jensen, for providing me with a project I truly enjoy, being a terrific bouncing board for ideas, and helping me to grow immensely as a researcher. I really appreciate his thoughtful guidance and support, as well as his ability to connect smaller project components with the larger picture.

I am grateful for all of my labmates in the Jensen group, who are always available for helpful discussions in the lab and make the work environment a happy and warm place to be.

I would like to thank my parents, my sisters Arielle and Bella, and my grandparents for being a constant source of encouragement, support, and love.

Lastly I would like to thank Ravi Netravali, my best friend and biggest inspiration.

Contents

List of Figures

List of Tables

Chapter 1

Introduction

1.1 Motivation

Every year over 30 billion metric tons of carbon dioxide is released into the atmosphere from anthropogenic sources.[1] Atmospheric carbon dioxide levels have reached nearly 400 ppm, and are projected to increase to 750 ppm by the end of the century.[2] Because of carbon dioxide's greenhouse gas properties and ocean acidification effects, these steadily increasing emissions pose significant concerns for climate change. Much work is being done to find solutions that address this problem, with efforts focused on minimizing economic and efficacy losses as compared to existing power infrastructures. These solutions generally fall under two categories: carbon capture, utilization, and storage (CCUS) and renewable energy technologies. The goal of CCUS is to capture CO_2 at a concentrated source or from the atmosphere, and then either upgrade it to useful products, or store it permanently through mineralization.[3,4] Renewable energy technologies aim to be either carbon-neutral, where energy is produced from carbon already in the carbon cycle (biofuels, waste-to-energy), or carbon-free, where no carbon dioxide is produced to generate energy (wind, solar, fuel cells, batteries, nuclear). Proposed large-scale solutions often involve a combination of many different approaches, as certain technologies are better suited to certain sectors, landscapes, and natural resources.

In the United States, the transportation sector accounts for 27% of the annual CO_2 emissions.[5] Globally, this sector accounts for 23% of annual CO_2 emissions, with a projected 70% increase by 2050 due primarily to growth of emerging economies.[6] Much research is being done in this area to reduce greenhouse gas emissions through renewable energy technologies, including fuel cells, batteries, and biofuels. While fuel cells and batteries have the potential to replace internal combustion engines in the future, they are currently plagued by low power densities and costs of up to 10 times that of engines. Even once these technologies meet the necessary technical and economic criteria, it would take time to see them implemented in a fleet-wide scale as engines phased out. Biofuels offer an attractive alternative because they can be implemented in the existing infrastructure with minimal changes to engine design and performance and fuel transportation and storage. When upgraded properly, these liquid phase, carbon-neutral fuels can directly supplement petroleum-derived gasoline and diesel.[7] Reports indicate that biofuels have the potential to reduce life-cycle greenhouse gas emissions by 77 to 115% as compared to petroleum gasoline.[8,9]

1.2 Overview of biofuels

Biofuel is produced through different chemical, biochemical, or thermal treatments of biomass, which has an average chemical composition of $C_6H_{10}O_5$. Biomass is a general term that can describe agricultural by-products, woody plants fallen by deforestation or natural causes, or dedicated energy crops.[6] In recent years work in this area has focused on generating ethanol primarily through fermentation of cellulosic biomass.[10] Because of challenges posed by competition with food sources, resource-intensive processing methods, and chemical and physical limitations of ethanol as a fuel, there is a growing interest in the production of biofuel through processing of lignocellulosic biomass, which does not compete with food sources and

requires low resource consumption during growth.[6] Other fuel molecules beyond ethanol are also being investigated in an effort to produce compounds with more suitable fuel properties. With the higher yields per hectare afforded by lignocellulosic biomass, the United States projects a 30% replacement of petroleum-derived fuels over the next 20 years, corresponding to 85 billion gallons of biofuels produced annually.[11] Development of efficient, low resource-intensive conversion technologies is imperative for the success of biofuel production and implementation.

Gasification and pyrolysis are the two thermal treatments used in the first step of processing lignocellulosic biomass to ultimately generate biofuels. Pyrolysis is preferred because it directly forms a liquid and has a higher heating value than the syngas product of gasification. Pyrolysis of biomass at temperatures between 450 and 550 °C yields about 70 wt.% oil with a lower heating value of 17 MJ/kg, and the balance permanent gases and char.[7] This bio-oil is a complex mixture of over 300 different compounds, with compositions dependent on the biomass feedstock and pyrolysis conditions. Fig. 1-1 breaks down the families of compounds present, the biomass portion responsible for their formation, and their respective weight percent ranges.

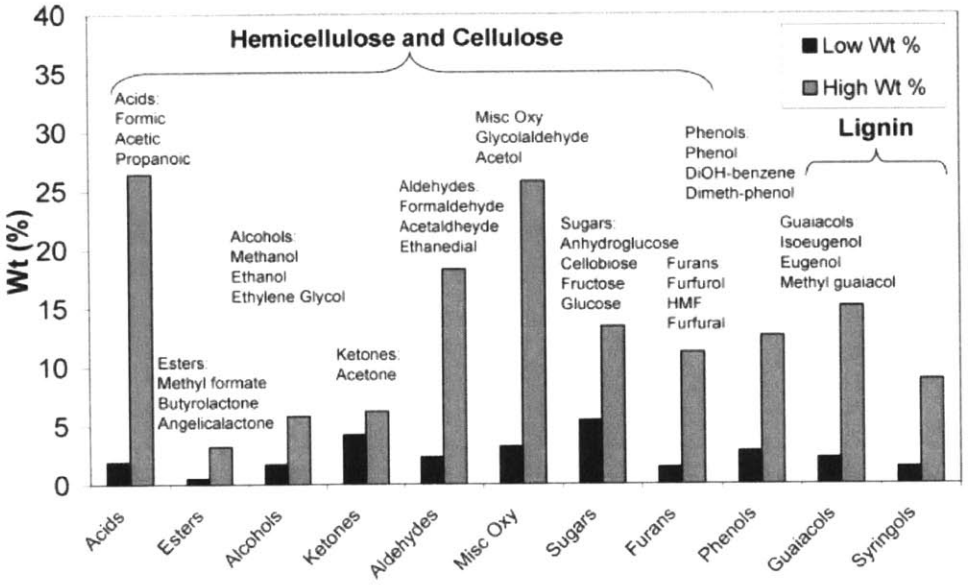

Figure 1-1. Percent (by weight) of different families of bio-oil compounds.[12]

Much like petroleum crude oil, bio-oil needs to be processed in order to generate gasoline and diesel molecules, which are also complex mixtures composed of C_6 to C_{20} compounds. Some of these compounds include straight chain and branched alkanes, alkenes, napthenes, and aromatics, which together have an average lower heating value of 44 MJ/kg and an average chemical composition of $C_nH_{1.87n}$. With its high acidity (pH 2-3), viscosity, polarity, and thermal instability, however, upgrading bio-oil poses significant challenges compared to the well-established practice of upgrading crude oil.[7,13]

1.3 Upgrading bio-oil to biofuels

1.3.1 Bio-oil deoxygenation

The first main goal of upgrading bio-oil is to remove oxygen to increase the energy density as well as the stability. While crude oil has virtually no oxygen, bio-oil is between 40-50 wt.% oxygen, both in the form of oxygenates and water (20-50 wt.%).[7]

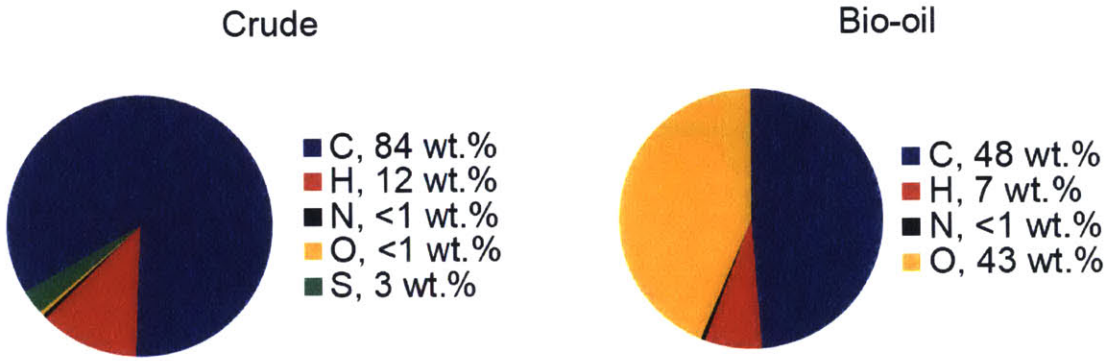

Figure 1-2. Elemental composition of crude oil compared to a bio-oil produced from fast-pyrolysis of switchgrass.[14]

These oxygenates are highly reactive and corrosive, and without further processing cause issues in storage, transportation, and combustion. Main approaches to remove oxygen from the bio-oil include dehydration, hydrogenation, and hydrolysis. One of the many challenges is that

these oxygen-removal strategies all require H_2, of which there is no large-scale renewable source.

1.3.2 Carbon-carbon bond synthesis

The second main goal of bio-oil upgrading is carbon-carbon bond synthesis between the low molecular weight compounds. As high as 85 wt.% of bio-oil is composed of molecules with a carbon number less than 6, yet the same percentage of gasoline molecules have a carbon number of 6 or higher.[15] Diesel molecules are significantly larger, in the C_{10}-C_{24} range.[16] The lower molecular weight compounds in bio-oil have a low energy density and do not have the physical and chemical properties necessary for liquid fuel storage or combustion in vehicle engines. In upgrading bio-oil, acids, alcohols, aldehydes, and ketones are the target molecules for carbon-carbon bond synthesis not only because they comprise a bulk of the low molecular weight compounds, but also because they are particularly reactive, volatile, and sometimes toxic oxygenates that need to be eliminated from the feed.

One of the main challenges of building a carbon backbone is that many industrially relevant reactions for synthesizing carbon-carbon bonds involve halides, as in Suzuki coupling and the Grignard reaction.[17] It is undesirable to introduce halides to the bio-oil system because they would further complicate an already complex chemistry and ultimately would need to be removed to maintain combustion and emissions standards downstream. Furthermore, many of these reactions require precious metals like palladium as catalysts.[17] Using such materials would decrease the economic competitiveness of biofuel compared to petroleum fuels.

Aldol condensation is a well-established reaction that synthesizes carbon-carbon bonds between aldehydes and ketones without going through a halide-mediated mechanism. An

overview of the general reaction scheme, shown between a ketone and an aldehyde, is illustrated in Figure 1-3.

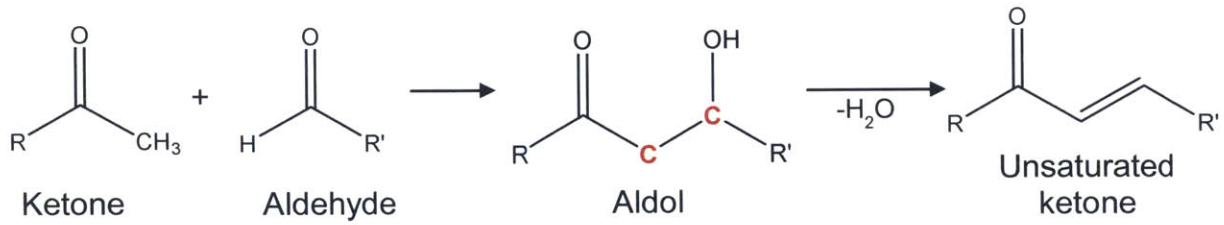

Figure 1-3. Schematic of the aldol condensation reaction.

Aldol condensation is particularly attractive to the bio-oil upgrading application because it targets the light ketones and aldehydes that are present anywhere from 7 to as high as 23 wt.% of bio-oil.[12] The most prominent compounds in these families are only in the C_1-C_3 range, as shown below.

Compound	Molecular Formula	Wt.% in bio-oil
Acetaldehyde	C_2H_4O	0.1 – 8.5%
Acetone	C_3H_6O	2.8%
Ethanedial	$C_2H_2O_2$	0.9 – 4.6%
Formaldehyde	CH_2O	0.1 – 3.3%
Methyl Ethyl Ketone	C_4H_8O	0.3 – 0.9%
Propanal	C_3H_6O	0.05%
Propenal	C_3H_4O	0.6 – 0.9%

Table 1-1. Aldehydes and ketones present in bio-oil from pyrolysis of biomass.[15]

In addition to upgrading the ketones that are present in the bio-oil after pyrolysis, aldol condensation can also target the ketones generated from other upstream upgrading techniques. In an effort to reduce the acidity of the bio-oil, much work[18] has been done to convert the phenolic

compounds and organic acids into less corrosive compounds. Selective phenol hydrogenation converts the reactive and solid-forming phenols into ketones, which can then be coupled in an aldol condensation with a lighter aldehyde or ketone to generate a larger molecule. The ketonization of organic acids, which can compose as much as 33 wt.% of bio-oil, yields ketones that could also be incorporated into the overall carbon coupling scheme as shown in Figure 1-4. Ketonization of acids is a viable approach to upgrading bio-oil, because it not only addresses the corrosive acids present, but also creates carbon-carbon bonds to yield larger ketones.

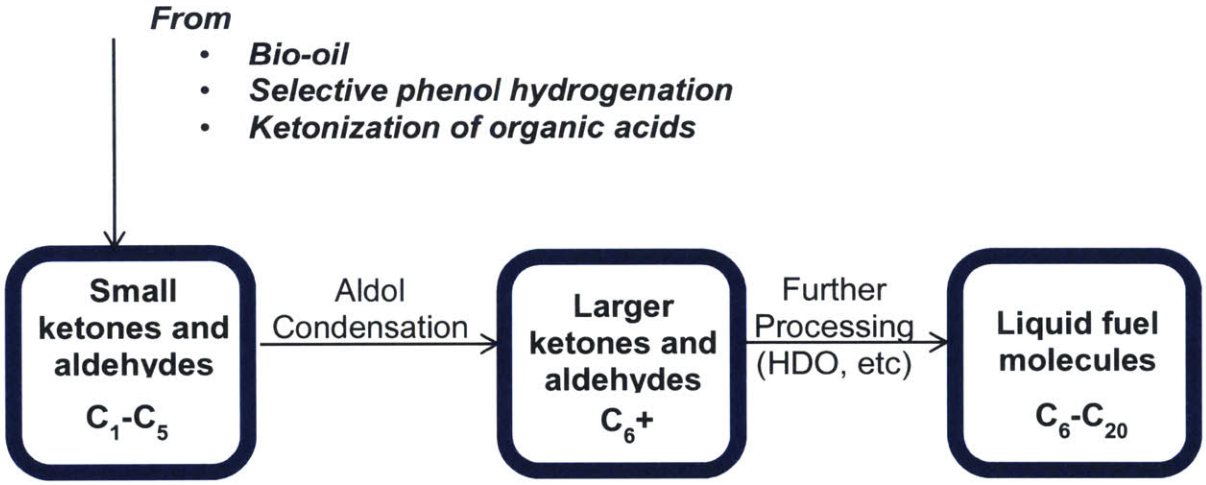

Figure 1-4. Scope of aldol condensation in the upgrading of low molecular weight ketones and aldehydes.

Derivatives of condensation reactions between carbonylic species include Michael addition, Tischenko addition, Knoevengael condensation, and Claisen condensation. The Michael reaction involves a similar enolate-intermediate base-catalyzed mechanism (as described in the following chapter), but this condensation is less attractive than the aldol reaction because it preserves all of the oxygen present in the reagents, which is undesirable for synthesizing fuel molecules both for reactivity and energy density reasons. The Tischenko reaction condenses two aldehydes or an

aldehyde with a ketone, but the resulting product is a carbonylic ester, which is also undesirable for fuel chemistries. Both the Michael and Tischenko reaction products could of course be deoxygenated in downstream processing, but ideally deoxygenation is kept at a minimum to reduce the consumption of hydrogen. The Knoevenagel reaction is a modified aldol condensation, in which a ketone or aldehyde reacts with a reagent containing an electron-withdrawing group, which could manifest as a carbonyl, nitrile, halogen, or nitro group. These other functional groups are not present in bio-oil chemistries, so the only relevant Knoevenagel reaction is the aldol condensation. The Claisen condensation involves carbon-carbon bond synthesis between carbonylic esters, which are indeed present in bio-oil. They represent a much smaller quantity of bio-oil (less than 5 wt.%), however, so the primary aldol condensation targets a larger range of the bio-oil chemistry. Because of this, much work has been done to investigate potential catalysts and reaction parameters for successful coupling of bio-oil model compounds in an aldol condensation reaction. This is the reaction utilized in this work.

Chapter 2

The Aldol condensation reaction

2.1 Reaction mechanisms and catalysis

2.1.1 Base-catalyzed mechanism

Aldol condensation involves either a self-condensation between two identical ketones or aldehydes, or a cross-condensation between two different molecules. The product is either an α,β-unsaturated ketone or aldehyde depending on the mechanism that is used. The reaction is primarily catalyzed by bases. Historically, catalysts have been homogenous liquid bases like NaOH, but more recently have moved towards solid bases like metal oxides and alkaline earth metals because of the advantages heterogeneous catalysis offers. This reaction takes place in batch at moderate temperatures, ranging from 0 to 150 °C, with reaction times anywhere from a few hours to on the order of days. The chemistry of the Bronsted base-catalyzed mechanism is below for an aldehyde self-condensation, although the mechanism can easily be extended to a cross-condensation or ketone self-condensation.

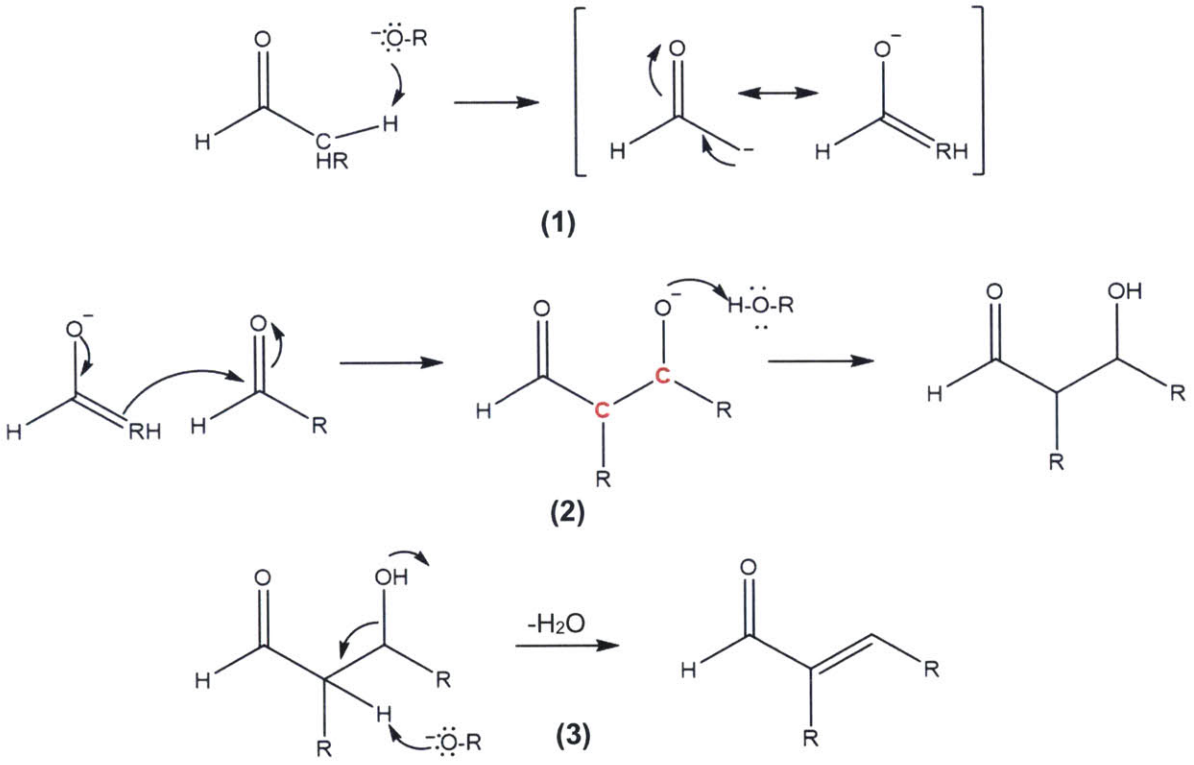

Figure 2-1. Base-catalyzed mechanism for aldol condensation of a generic carbonyl compound.

In the first step **(1)**, the base deprotonates the α-carbon, which in resonance forms the more stable enolate isomer.[19] The nucleophilic double bond of the enolate ion will attack the carbon of the carbonyl group of another aldehyde **(2)**, which is electrophilic in this functional group. The new double bond is formed between the two carbons as denoted in red. The excess negative charge on the non-carbonyl oxygen will then deprotonate the basic catalyst protonated in the first step, regenerating the catalyst. The product is the "aldol", named for having both aldehyde and alcohol functional groups, with a carbon number equal to the sum of the starting aldehydes or ketones. Step **(3)** is a dehydration step: the basic catalyst will deprotonate the α-carbon again, but rather than stabilizing the carbanion through enolization, the hydroxyl group is

removed and the two neighboring carbanions form a double bond. The result is an unsaturated aldehyde.

2.1.2 Acid-catalyzed mechanism

While the reaction is historically catalyzed by bases, there is an acid-promoted mechanism as well. The chemistry of the Bronsted acid-catalyzed mechanism is shown below. It is again shown for a self-condensation of an aldehyde, but applies similarly to a ketone self- or cross-condensation.

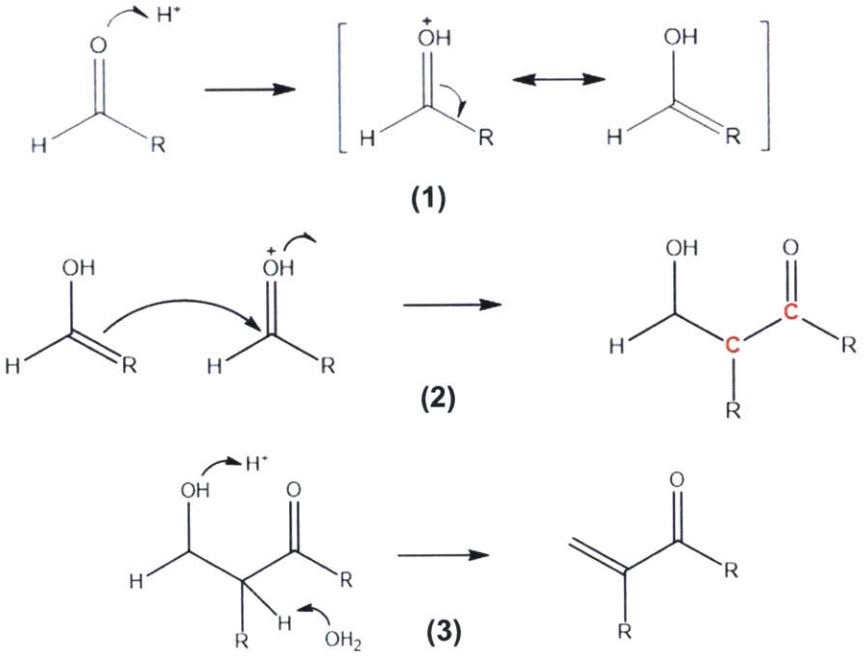

Figure 2-2. Acid-catalyzed mechanism for aldol condensation of a generic carbonyl compound.

In step **(1)** of the acid-catalyzed mechanism, the acid catalyst protonates the carbonyl oxygen, generating the enol intermediate. Consequently, the enol attacks the carbon of the carbonyl group on another protonated aldehyde **(2)**, which has an even larger positive charge density due to the protonation of the carbonyl oxygen. Upon deprotonation of this oxygen, an

aldol is formed with a synthesized carbon-carbon bond as shown in red. In step **(3)**, a water molecule deprotonates the α-carbon to regenerate the acid (ie, hydronium) catalyst, while the hydroxyl group is protonated simultaneously. The resulting molecule will dehydrate to eliminate both the over-coordinated oxygen and unstable α-carbanion. The resulting molecule is an unsaturated ketone.

2.1.3 Cooperative acid-base mechanism over solid catalysts

While base-only and acid-only catalysts are active in promoting aldol condensation, it has been shown by several authors that there also exists a cooperative acid-base mechanism that promotes the reaction.[20-24] The chemistry of the bifunctional catalyst-promoted mechanism is shown below for a generic self-condensation.

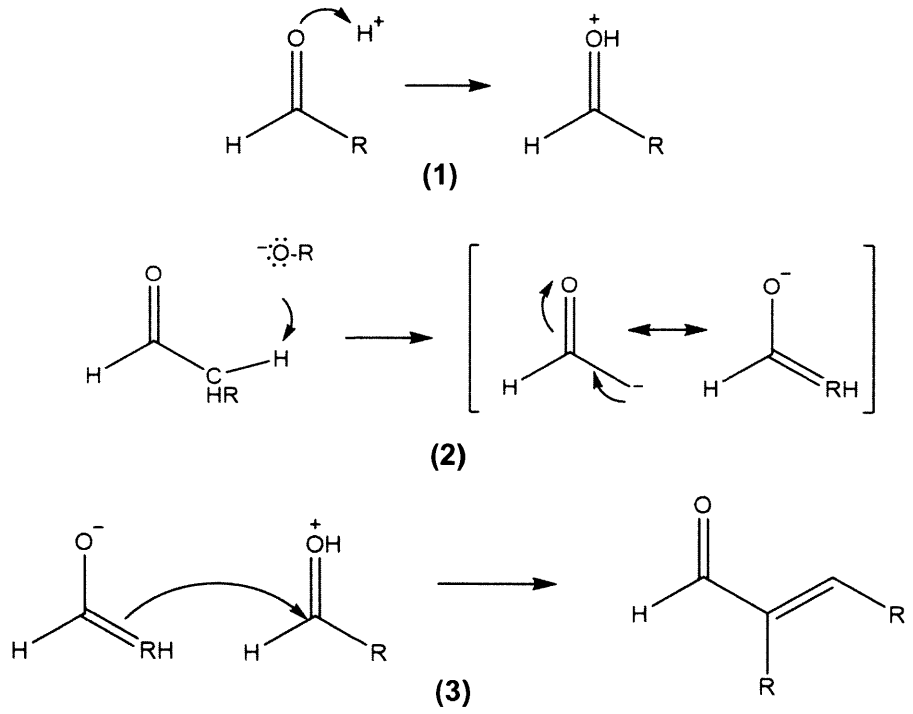

Figure 2-3. Proposed acid-base-catalyzed mechanism for aldol condensation of a generic carbonyl compound.

The acid site first activates the oxygen of the carbonyl group, increasing the electrophilicity of the carbonyl carbon **(1)**. In step **(2)**, the basic site deprotonates the α-carbon, generating the carbenium anion in resonance with the enolate anion. The nucleophilic enolate anion then attacks the activated compound, yielding an aldol, which dehydrates into an unsaturated α,β-unsaturated aldehyde or ketone **(3)**. Both Bronsted and Lewis-type acidic and basic sites are active in this reaction.[23]

2.2 Related work

Homogenous catalysts like NaOH and H_2SO_4 proceed respectively through these base and acid-catalyzed mechanisms for the aldol condensation reaction. Heterogeneous catalysts can similarly promote the reaction through different types of Bronsted and Lewis basic and acidic sites. In addition to the benefits of separation and recycling, heterogeneous catalysts are also advantageous because unlike homogenous catalysts, they can simultaneously have acidic and basic sites through physical separation, allowing the bifunctional mechanism to take place.

2.2.1 Base-only and acid-only catalysts

Di Cosimo et al.[19] investigated the vapor-phase aldol condensation of acetone, a good model compound for bio-oil, over MgO and MgO-promoted catalysts, doped with either alkali (Li, Na, K, Cs) or alkaline earth (Ca, Sr, and Ba) metal ions. The reaction took place in a flow reactor with a H_2 to acetone ratio of 12 to 1 (by mole) at 300 °C. For both unpromoted and promoted MgO, the primary active sites in the aldol condensation are low-coordinated surface O^{2-} anions, which act as Bronsted bases to deprotonate the α-carbon. The authors found a good correlation between rate of reaction and number of basic sites on the catalyst, suggesting that the rate-limiting step for acetone condensation is the base extraction of an α-hydrogen. In this work,

the dimer, mesityl oxide, was the primary product, and the highest condensation product generated was the trimer, phorone, which was readily converted to the cyclic ketone, isophorone. Further condensation between isophorone and acetone was not observed, nor were conversions of acetone higher than 20%. Catalysts with different types of active sites were studied by other authors that include hydroxyl groups of weak base strength on oxides and hydrotalcites, as well as coordinated Metal-O^{2-} sites of medium base strength on metal oxides.[23–25]

Acid-catalyzed aldol condensation of propionaldehyde, carried out in flow with a H_2 to C_3H_6O ratio of 17500 (by volume), was examined by Hoang et al.[14] over two different H-ZSM-5 zeolites with bridged hydrogen as the active Bronsted acid sites. Over the H-ZSM-5 with Si to Al ratio of 45 and at 400 °C, conversion of propionaldehyde reached 100% at a space time of 15 minutes. These reaction conditions produced yields of approximately 52% aromatics, 38% light gases (C_1-C_3), and 10% isoalkenes (C_4-C_9), with the cyclized trimer being the primary aromatic compound. The aldol condensation is responsible for these higher molecular weight compounds, while disproportionation and cracking catalyzed by the active acid sites cause a significant portion of the aldol products to generate the C_1-C_3 light gases. Reduction in reaction temperature was shown to reduce these undesirable secondary reactions, but conversions and desired condensation yields suffered as a result.

2.2.2 Bifunctional catalysts

Ordomsky et al.[26] investigated the conversion of acetaldehyde, perhaps the best model carbonyl for bio-oil both for its high concentration and reactivity, over SiO_2-supported MgO and ZrO_2 catalysts. Both catalysts had basic sites from low coordinated surface O^{2-} anions, but also contained significant quantities of Lewis acid sites due to several factors: dehydroxylation of ZrO_2 during calcination yielding exposed Zr^{4+}, low-coordinated surface Mg^{2+}, and the OH

groups present on the SiO_2 support. The authors found through targeted CO_2 and pyridine site poisoning that these acidic sites, rather than the basic sites, were involved more in the condensation of acetaldehyde. The reaction was carried out at 130 °C at atmospheric pressure, with no excess H_2 flow. At the same conversion, selectivity to the acetaldehyde dimer, crotonaldehyde, was 87.6 and 83.4% for MgO and ZrO_2, respectively.

In the batch runs of acetone condensation at room temperature over an activated Mg-Al layered double hydroxide (LDH) catalyst, Lei et al.[27] obtained a maximum conversion of 23% at 300 minutes and reaction temperature of 0 °C. LDH calcined and activated through rehydration possess OH pairs with a fixed separation that act as acid-base pairs.

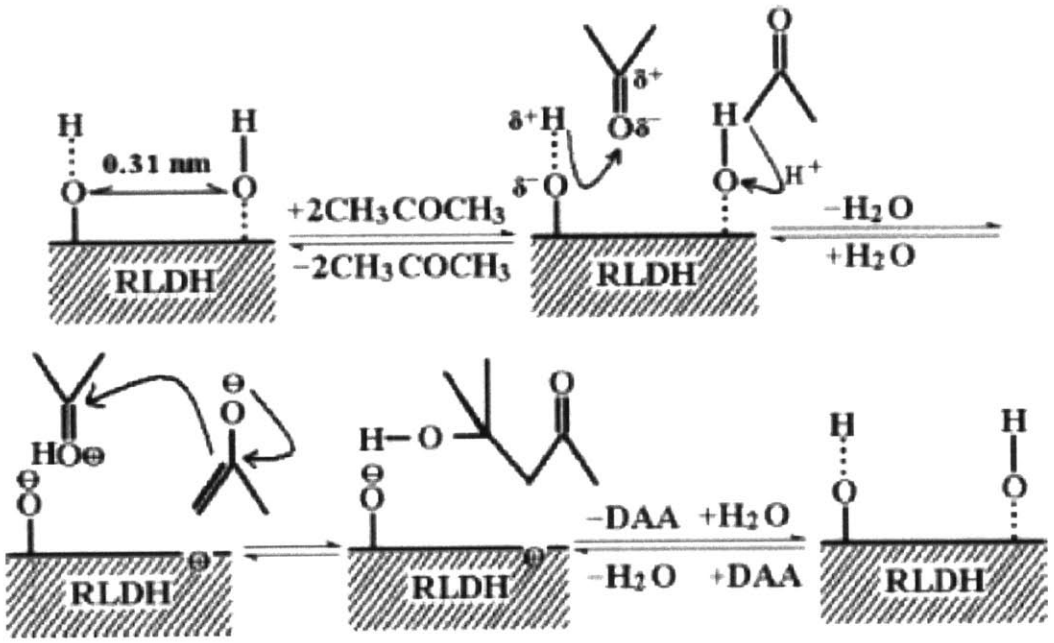

Figure 2-4. Mechanism for rehydrated LDH with bifunctional hydroxyl group pairs.[27]

One of the hydroxyl pairs acts as a Bronsted base, deprotonating the α-carbon of an acetone molecule to generate the enolate anion. The neighboring site serves two functions: as a Bronsted acid, it protonates the oxygen of another acetone molecule to polarize the carbonyl group, while

also localizing the activated group next to the enolate, better facilitating the nucleophilic attack. The primary product was diacetone alcohol, the aldol of the acetone dimer. Consistent with other work, the dehydration to mesityl oxide did not take place due to the low temperature of reaction.[28]

The high pressure, liquid-phase aldol condensation of three bio-oil model compounds was carried out by Snell et al.[20] using $AlPO_4$ and nitrated $AlPO_4$ catalysts in batch. The P-OH groups acted as weak Bronsted acid sites that polarize the carbon-oxygen bond in one carbonyl molecule. This polarization increased the carbonyl carbon's susceptibility to attack by the enolate intermediate of another carbonyl compound, which formed from the relatively weak Lewis basic sites corresponding to bridged oxygen.[29] Reactions involved the condensations between acetaldehyde and acetone, and acetaldehyde and MEK, to investigate the effects of catalyst acidity and basicity on preferential yields towards the self or cross condensation products. At 150 °C and 25 bar of N_2 overpressure, the acetaldehyde dimer and the cross condensation products between acetaldehyde and the two ketones ((3-methyl-)3-penten-2-one, 4-hexen-3-one) were the only measurable products. Consistent with other work done in this area, the self-condensation product is favored for increasing catalyst basicity, while the acid sites promote cross-condensation.[30]

Other authors investigated bifunctional mechanisms involving Lewis acid and Bronsted basic sites of MgO, as well as mixed oxides containing Ce, Al, Co, and Ti, with different sites and mechanisms associated with varying compositions and synthesis method.[24,30]

2.2.3 Limitations of existing work

The work that has been done to date with aldol condensation of bio-oil model compounds illustrates several issues that pose concerns regarding its feasibility in the bio-oil upgrading scheme: carbon number limitations, industrially unfavorable processes, and excessive hydrogen consumption.

As shown in the literature, the self-condensation of acetaldehyde yields the C_4 dimer crotonaldehyde, which is advantageous in that with its significantly higher boiling point, is a liquid at ambient conditions. However, crotonaldehyde is still too light for appreciable implementation as a supplement to petroleum gasoline and diesel fuels: less than 3 wt.% of gasoline contains C_4 alkanes which form as by-products from catalytic naphtha cracking, while diesel combustion requires fuels with a minimum carbon number of 9.[16] Ordomsky et al .[26] observed a second condensation between acetaldehyde and crotonaldehyde to produce the trimer, sorbaldehyde, but it was not generated in significant yields: selectivity to crotonaldehyde was over 80% for both catalysts investigated. Similarly, Di Cosimo et al.[19] observed the cyclized trimer as the highest acetone condensation product, which yields the sufficiently large C_9 compound. However, yields of the trimer were low, as was overall conversion. Hoang et al.[14] achieved 100% conversion of propionaldehyde in only 15 minutes, with yields towards C_6-C_9 condensation products over 50% and the highest selectivity to the trimer. However, the acidic sites also promoted the cracking reaction to produce nearly 40% yields of undesired light gases (C_1-C_3).

Using the bio-oil model compounds listed in Table 1-1, the theoretical maximum carbon number would be 8 from the self-condensation of MEK. However, the C_8 dimer has not been observed to form to an appreciable extent.[20] Additionally, MEK, along with propionaldehyde and

propenal, are not as representative of bio-oil carbonyl compounds as formaldehyde, acetaldehyde, ethanedial, and acetone, so should not be the focus of condensation reactions with respect to practical implementation. For this process to be considered a viable pathway to bio-oil-derived biofuel, synthesizing sufficiently high molecular weight compounds is fundamental.

Finally, aldol condensation is typically run in mild conditions with long reaction times in batch reactors. Because scale-up and production rates favor continuous flow systems substantially, it is of interest to investigate if favorable conversion and yields are achievable in flow. Additionally, in order for renewable energy technologies to be considered for large-scale implementation, they must compete economically to an extent with existing infrastructures, and obviously require less resource consumption and waste generation in both development and end use. As a result, it is imperative that high pressures and large H_2 consumption are avoided to minimize the excessive energy and financial costs associated with these conditions.

The goals of this work are two-fold: (1) to produce fuel range molecules from prevalent model compounds; (2) to achieve reasonable conversion in a flow system.

Chapter 3

Bifunctional acid-base materials for polycondensation of acetaldehyde

3.1 Materials in literature

It has been shown in the literature that low molecular weight ketones and aldehydes, primarily acetone, formaldehyde, and acetaldehyde, can combine in multiple aldol condensations to yield their respective trimers, tetramers, and higher condensation products.[31-33] The reactions with aldehydes in particular, which are generally more reactive than their ketone counterparts, proceed rapidly and produce high molecular weight compounds, as discussed in the following sections. If this multiple condensation reaction, or "polycondensation", could be truncated to produce high yields of intermediate polycondensation products in the C_6 to C_{20} range, it could provide a feasible pathway for bio-oil upgrading into biofuels. To achieve the first goal of this work, the first step was to examine which materials could catalyze this polycondensation. From there catalysts with similar active sites could be evaluated for bio-oil model compound polycondensation in the flow system developed, as described in the following chapter. Acetaldehyde is chosen as the model compound to examine in the polycondensation reaction for several reasons. First, it is usually the most prevalent carbonyl compound in bio-oil, with a maximum at 8.5 wt.%. This might not seem like a substantial percentage, but considering that

bio-oil can have over 300 different compounds falling into over 6 different families of functional groups, it is a sizable amount for one compound to represent. Additionally, acetaldehyde is particularly reactive both with itself and other functional groups, and with a boiling point at room temperature, it poses significant challenges for bio-oil stability and transportation.

In the photocatalytic oxidation of ethanol over Evonik (formerly Degussa) P25 TiO_2, acetaldehyde is formed as an intermediate. It has been observed by Luo and Falconer[33] that the catalyst is deactivating due to the trimer and high molecular weight compounds depositing on the catalyst surface due to polycondensation of the aldehyde. This reaction is observed even in the absence of UV light. P25 TiO_2 is a biphasic mixture of anatase and rutile in 75 ± 5% and 25 ± 5%, respectively.[33] When the authors compared acetaldehyde condensation over pure anatase and P25 TiO_2, they found that over the P25 the trimer and higher condensation products formed. On the anatase alone, however, only the dimer was observed. Comparing the differences between these two materials showed that the P25 has significantly more acid sites, which result in a much higher surface adsorption of acetaldehyde and promote the acid-base mechanism. Additionally, the P25 has more active sites overall compared to the anatase.

Ordomsky et al.[26] similarly found that Lewis acid groups present in a ZrO_2/SiO_2 catalyst are responsible for the adsorption of acetaldehyde on the surface, through interactions of the carbonyl oxygen with low-coordinated Zr^{4+} sites. The presence of these acid sites further promotes the aldolization of acetaldehyde because the basicity of the neighboring lattice oxygen increases due to the Lewis acid-carbonyl oxygen attraction. The stronger basicity favors the abstraction of the α-hydrogen. Additionally, Bronsted acidity provided by hydroxyl groups adsorbed on the silica support allow H-bonding between hydroxyl hydrogen and a second acetaldehyde carbonyl group. This increases the positive charge density on its carbonyl carbon

and encourages the nucleophilic attack by the oxygen. The mechanism as proposed in Fig. 3-1 for P25 TiO_2 is similar to that proposed for ZrO_2/SiO_2.[26] It is possible that the acid sites responsible for the carbonyl activation and increase in acetaldehyde adsorption promote a polycondensation reaction.

In light of this, catalysts with acid-base bifunctionality are of interest in this work to achieve high molecular weight compounds from acetaldehyde. P25 TiO_2 is examined as a baseline case because of its established success in condensing multiple units of acetaldehyde over a range of temperatures.[33] Additionally, an activated hydrotalcite-like compound is investigated for activity in a polycondensation because it possesses acid-base pairs and has been shown to be active in standard aldol condensation reactions.[27,28] This material is abundant and relatively inexpensive, which is makes it attractive as well.

3.2 Active sites and mechanisms

3.2.1 P25 TiO_2

P25 TiO_2 is considered the standard in photocatalysis, and as a result much work has been done to identify the components that are active in promoting photocatalytic reactions.[34] Among its electrical conductivity and band gap features, its surface sites are of particular relevance to its success as a catalyst in polycondensation reactions. Like many transition metal oxides, TiO_2 has Lewis acid sites that arise from coordinatively unsaturated Ti^{4+} surface cations, and Lewis basic sites from low coordinated O^{2-} surface anions.[35] Additionally, P25 TiO_2 crystallites, which are sold as a nanopowder (average 21 nm particle size), have surface roughness that contributes to cationic and anionic sites on edges, corners, and steps with even lower coordination. The lattice oxygen of P25 TiO_2 is much weaker than that of alkaline earth

metal oxides.[35] As a result, it is proposed[35,36] that primarily defect oxygen sites are sufficiently basic to deprotonate the α-carbon in the aldol condensation mechanism, as on the (001) and (010) surfaces. On these planes, Ti^{4+} and O^{2-} are especially strong Lewis sites.[35]

Both independent anatase and rutile phases adsorb molecular water significantly. P25 TiO_2 adsorbs water both molecularly and dissociatively, resulting in extensive surface hydroxylation. These hydroxyl groups also play an important role in P25 TiO_2's catalytic properties, as they can act as both Bronsted acids and bases.[36] It is proposed that when the P25 TiO_2 surface is hydrated, these hydroxyl groups have sufficient Bronsted basicity to execute the deprotonation in the aldol condensation mechanism. A mechanism for acetaldehyde condensation on the surface of P25 TiO_2 is below, as proposed by Singh et al.[37] In this mechanism, lattice oxygen is sufficiently basic to remove the α-hydrogen and create the enolate intermediate, so this could be taking place on a defect site on one of the highly active crystal planes, namely 010.[35,36]

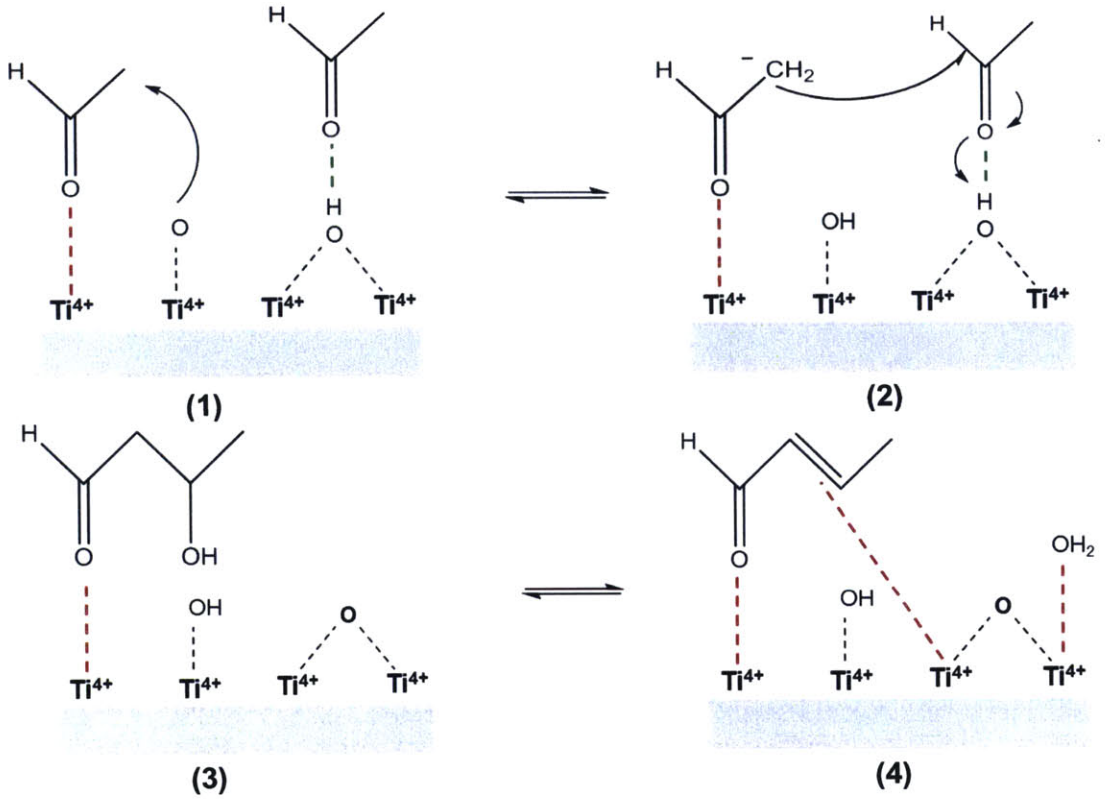

Figure 3-1. Proposed mechanism[37] of acetaldehyde condensation on the surface of P25 TiO_2.

In this mechanism, an acetaldehyde molecule will adsorb onto a strong Lewis acid site of the P25 TiO_2 surface through its carbonyl oxygen group. A neighboring lattice oxygen of sufficient basic strength will deprotonate the α-carbon of the adsorbed acetaldehyde, generating a carbenium anion which will in resonance form the enolate intermediate. Simultaneously, another unit of acetaldehyde will adsorb through hydrogen bonding onto a surface hydroxyl group **(1)**. This hydrogen bonding increases the positive charge density of the carbonyl carbon because of the oversaturated carbonyl oxygen, which aids in the neighboring enolate anion's nucleophilic attack **(2)**. The aldol is formed, and is stabilized on the surface still through oxygen carbonyl-Ti^{4+} surface attraction **(3)**. The dehydration in step four results in a water molecule that preferentially adsorbs on a neighboring Ti4+, which then dissociates the molecule and regenerates the surface hydroxyl group. The dimer, crotonaldehyde, is formed. It is stabilized as an adsorbed product

both by the oxygen-Ti^{4+} and double bond-Ti^{4+} interactions **(4)**. It is possible that this interaction is one of the reasons this material is active in a polycondensation. Rather than desorbing and leaving the bed as the dimer, the product stays adsorbed because of the double bond-strong Lewis acid site attraction to react with another unit.

3.2.2 Hydrotalcite-like compounds

Hydrotalcite-like compounds (HTlc) are structurally similar to the naturally found mineral hydrotalcite ($Mg_6Al_2CO_3(OH)_{16} \cdot 4H_2O$). These materials have metal hydroxide sheets with an octahedrally coordinated M^{II} metal as in brucite, with anions and H_2O molecules intercalated between layers. Also known as layered double hydroxides or synthetic anionic clays, they have a general chemistry of $[M^{II}_{1-x}M^{III}_x(OH)_2]^{2+}(A^{n-})_{x/n} \cdot yH_2O$.[27] The substitution of an M^{II} with an M^{III} in the metal hydroxide layer generates a charge imbalance, which is compensated by anions in the interlayer galleries.[27] These materials are active as solid base and acid-base catalysts. Metals vary from various alkali earth metals to transition metals, including Mg, Ni, Al, Co, and Fe, while anions include CO_3^{2-}, OH^-, NO_3^-, and Cl^-.[28,38] HTlcs are of interest in many applications because different cations can be chosen during synthesis, and anions can be easily exchanged to functionalize the material with desired properties. Fig. 3-2 shows the interesting structure of these compounds.

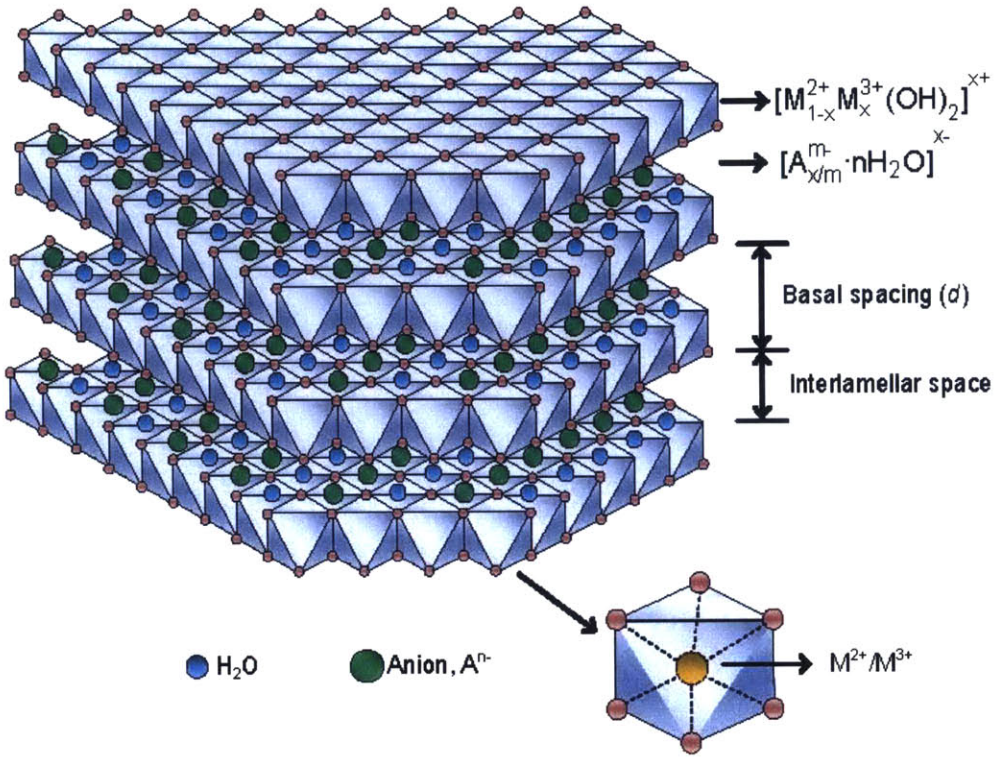

Figure 3-2. Anions in interlayer galleries maintain charge neutrality of the M^{III}-substituted M^{II}-hydroxide in a HTlc.[39]

When HTlc are calcined at temperatures of 500 °C and higher, they go through a phase transition in which they dehydrate, lose interlayer anions, and decompose in the brucite-like sheets, yielding a weakly crystalline oxide of the primary metal with substitutions of the secondary metal on its lattice.[40] These calcined oxides derived from HTlc have the interesting property of "memory effect", in that if dispersed in water with specified anions in solution at room temperature can regenerate the original layered structure with the initial or different anions in the interlayer galleries.[28,40] These rehydrated HTlc have been shown to be active catalysts possessing both acidic and basic sites.[28]

In this reaction mechanism, interlayer anions are hydroxyl groups. The preparation of this HTlc is discussed in the following chapter. Hydroxyl groups at a fixed distance apart on basal

surfaces act as Bronsted acid-base pairs, as shown in Fig. 3-3.[27] An acetaldehyde molecule diffuses to the catalyst surface and adsorbs through hydrogen bonding with the acidic hydroxyl group, polarizing this bond and increasing the positive charge density on the carbon **(1)**. The neighboring basic hydroxyl group initiates the aldol condensation mechanism by deprotonating another acetalehyde's α-carbon, producing the nucleophilic enolate intermediate which attacks the neighboring activated carbon **(1, 2)**. The aldol forms, stabilized by the acidic site **(3)**, which then dehydrates to yield the dimer, crotonaldehyde, regenerating the catalyst **(4)**. These sites are of medium-high Bronsted acidity and basicity.[27,41]

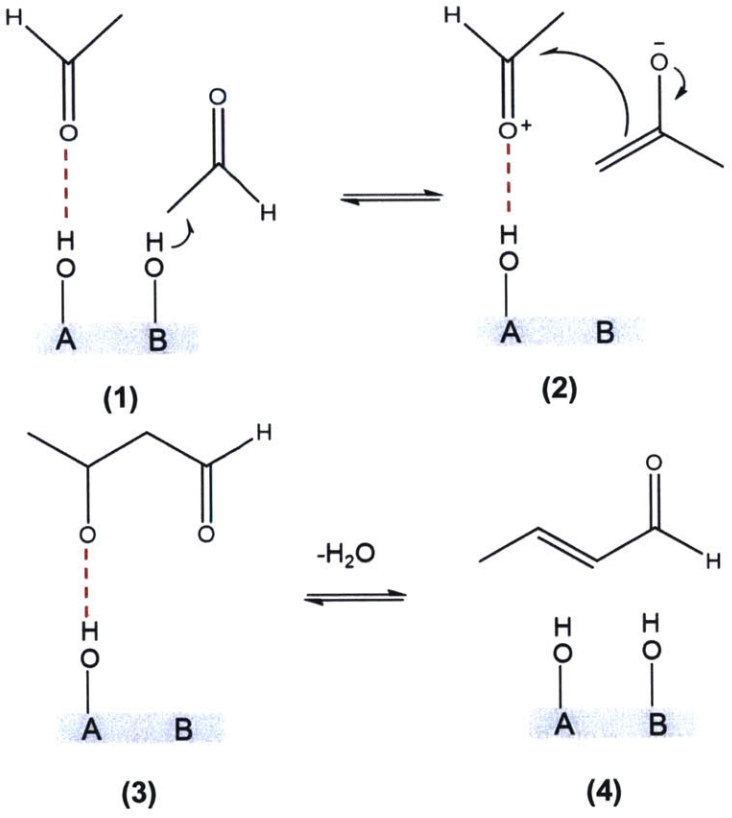

Figure 3-3. Proposed acid-base mechanism of neighboring hydroxyl pairs on basal surfaces of an activated HTlc compound.[27]

3.3 Polycondensation Chemistry

It is important to note that the aldol condensation reaction mechanism is well understood for single condensations (ie, in the formation of the dimer). However, as the unit compound begins to polycondense, subsequently higher condensations are not so straight forward and products need not be the theoretical linear product of the n-mer with another unit. In acetaldehyde polycondensation, the first two condensations yield the dimer, crotonaldehyde, and trimer, sorbaldehyde, for which the mechanisms are direct aldol condensations. Subsequent condensations yield heavier compounds that are so bound to the surface that even analysis through TPD, TPH, and TPO at high temperatures proves difficult.[33] Luo and Falconer[33] found that many of these compounds are aromatics and other cyclized chemistries. This is consistent with what Di Cosimo et al.[19] found in the polycondensation of acetone. The liner trimer phorone was formed but rapidly cyclized into isophorone. As a result, as C_8 and higher compounds begin to form, the chemistry is not well understood, but hopefully can be examined more closely moving forward in this work.

Chapter 4

Experimental Methods and Materials Characterization

4.1 Development of the Flow System

4.1.1 System goals

A flow system was designed to examine the performance of the acid-base catalysts described previously in the polycondensation of acetaldehyde. In addition to the transport phenomena and production rate advantages associated with a continuous reactor compared to batch, the flow design is an imperative component to the specific aims of this work. In batch conditions, acetaldehyde can either react to form its dimer or proceed through a polycondensation mechanism to form such heavy products that they are solids, as shown by Luo and Falconer[33] over P25 TiO_2. The goal is to control the polycondensation and truncate the reaction to terminate at 3 to 10 condensations to generate liquid-phase molecules in the gasoline and diesel range. To do this, a flow system is of interest because it offers significantly more control over the reactant-catalyst interaction through residence time. This interaction can also be controlled through tuning of the reactor bed itself, which is only capable in a flow system.

In designing the system, certain parameters were considered in order to develop a process step that would fit well into the overall bio-oil upgrading process. As mentioned earlier, bio-oil stability is a major challenge because of the reactive oxygenates. Ideally, a portion of these oxygenates would be addressed immediately upon exiting the pyrolysis unit, and these are targeted for the polycondensation.

Pyrolysis of biomass takes places between 450 to 550 °C, producing permanent gases, char, and predominantly oil, which forms from the condensation of pyrolysis vapors as they cool. In traditional crude oil processing, the oil is distilled and the distillate fractions are processed accordingly to produce gasoline and diesel-range molecules through catalytic hydrocracking. If bio-oil were distilled, light oxygenate vapors would boil off first, followed by water vapor. Rather than leaving an oil that could similarly be processed into shorter hydrocarbon chains, the distillation yields 40-60% carbonaceous solids that are unable to be further processed into liquid fuels.[42] Challenges posed by revaporization motivate the upgrading of the lightest fractions before they condense. The flow system in this work then is developed for gas phase reactions to simulate those that would be carried out in the post-pyrolysis step—upgrading of hot pyrolysis vapors. Additionally, the system is run at ambient pressure both to maintain the gas phase of the species that are present (many of which are near their phase transition conditions) and to avoid the high costs and risks associated with a high pressure system.

As mentioned earlier, co-feeding of hydrogen has been used in previous work[14,19,33] to help the polycondensation products desorb from the catalyst surface and exit the reactor bed in the gas or liquid phase. However, because there is no large-scale source of renewable hydrogen currently available, it is best economically and environmentally to avoid using hydrogen as a

means to desorb heavy condensation products. As a first investigation, no hydrogen is co-fed in this reaction.

4.1.2 System design

A schematic of the flow system designed to test the performance of P25 TiO_2 and the activated HTlc is shown in Fig. 4-1.

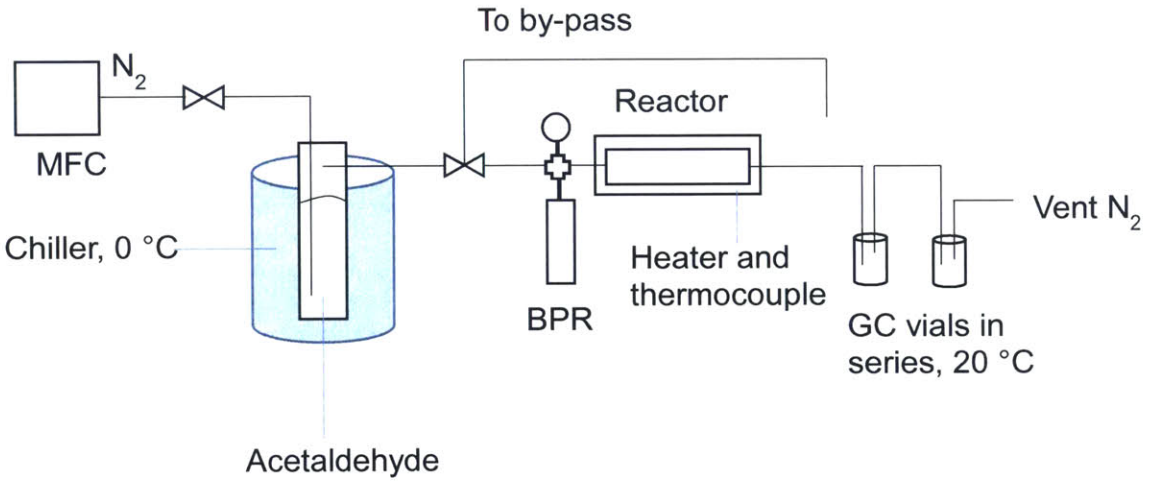

Figure 4-1. Schematic of flow system.

A Sierra MicroTrak 101 mass flow controller delivers N_2 at specified flowrates into a bubbler containing pure acetaldehyde (Sigma Aldrich, ACS reagent, ≥99.5%). The headspace of the bubbler is a mixture of N_2 and acetaldehyde, which is driven downstream by the inlet flow of N_2 into the liquid. The total flowrate through the system is measured with a low-flowrate capillary bubblemeter after steady state is achieved after every setpoint change. The concentration of acetaldehyde in the headspace is a function of its vapor pressure, so to control this the bubbler is maintained at 0 °C by a chiller. The outlet line is directed into a cross union, with the outlet to the reactor bed. The other two lines go to a pressure gauge (maximum P = 6 bar) to measure pressure drop across the packed bed for use in the Ergun equation, and to a pressure-relief valve,

which is a back pressure regulator rated at 75 psig cracking pressure in case clogging resulted in pressure spikes dangerous to the system or general safety. Two poppet check valves serve a similar purpose so as to prevent backflow into the bubbler as well as into the mass flow controller. All lines except the reactor inlet and outlet are made of $^{1}/_{16}$" PEEK tubing (0.03" ID) for chemical compatibility and strength under high pressures.

The packed bed reactor is an electropolished stainless steel tube from Swagelok fitted with a Valco nut/ferrule on either end that connect to $^{1}/_{16}$" stainless steel tubing. The reactor bed is heated by two heating cartridges placed into a metal chuck which gets secured around the bed. To maximize heat transfer to the bed a layer of graphite paper is wrapped around it so there is a snug fit within the chuck. A picture of the bed shown in Fig. 4-2.

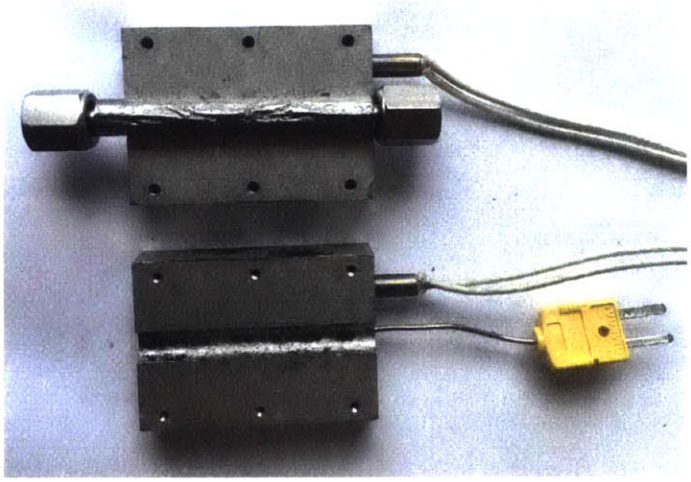

Figure 4-2. Reactor bed with cartridge heaters, heating chuck, graphite paper, and thermocouple.

A 2μm frit is placed in each of the Valco internal nuts (reactor inlet and outlet) to prevent the catalyst from escaping the bed and clogging the lines.

The effluent of the reactor is well insulated to prevent inline condensation of condensation products, and flows directly into a 2 mL GC vial (Agilent). This vial contains a

specified amount of toluene as a solvent and dodecane as a calibration standard. Toluene was chosen because it is non-reactive with acetaldehyde and the two are miscible. Unconverted acetaldehyde and any products formed bubble into the toluene and condense. While all condensation products are liquid at room temperature (the smallest product, the dimer, boils at 104 °C), not all of the acetaldehyde is captured in the first stage of collection (boiling point = 20 °C). The first vial is then vented to a second GC vial, again containing toluene and dodecane, to capture any uncondensed acetaldehyde from the first stage. In fact, the back pressure induced by the small-ID tubing between the second and first stages is sufficient to keep over 97% of the acetaldehyde in the first stage. The second vial is vented to atmosphere to release the N_2 so as not to pressurize the system. The initial method was to collect the acetaldehyde in a vial kept in a dry-ice acetone bath at temperatures between -55 and -65 °C. However, this method was abandoned because the acetaldehyde was condensing in the inlet needle, preventing collection in the vial itself. Additionally, such low temperatures might induce solidification of condensation products. The two-stage collection method at room temperature avoids such issues.

Reagent and products are analyzed offline in the liquid phase using an Agilent GC-FID/MS fitted with a HP-5 column. System specifications are outlined in Table 4-1.

Sierra MicroTrak 101 mass flow controller	0.100 – 4.000 mL/min
Reactor bed volume	0.731 mL
Reactor bed dimensions	3 mm ID x ¼" OD x 100 mm L
Residence time range	10 s – 5 min
Cartridge heaters maximum temp.	400 °C

Table 4-1. Specifications of the flow system developed.

For conversion calculations, the standard definition is used:

$$X = \frac{C_{A,0} - C_A}{C_{A,0}},$$

where $C_{A,0}$ is the initial concentration as measured through the bypass, and C_A is the concentration measured after the reaction.

4.2 Materials Preparation and Characterization

4.2.1 Pelletized P25 TiO_2

Commercial P25 TiO_2 by Evonik is only sold as a nanopowder with average particle size of 21 nanometers. To avoid the issues with packing and associated pressure drop that would arise with nanoparticles in a packed bed, it was necessary to create larger particles that could then be uniformly sized. A recipe was found in the literature[43] that creates large pellets of P25 TiO_2 from the commercial nanopowder. One milliliter of distilled water was added to every 1 gram of P25 TiO_2. The mixture creates a sticky material that was then extruded and dried at 110 °C for 12 hours to remove excess water. The dried mixture yields large pellets that can then be crushed gently with a mortar and pestle and sieved. Molecular test sieves of 120 and 200 mesh were used to keep particles with diameters between 75 and 125 μm. This size range promotes high surface area and minimal packing. The sample prepared in this way will be identified as pelletized P25 TiO_2.

It was important to validate that the preparation method as described above did not significantly affect the features of P25 TiO_2 that make it such an active catalyst in acetaldehyde condensation. To ensure that adding water and drying the material affected neither the crystalline composition nor the crystalline size, x-ray diffraction (XRD) was run on both the nanopowder and the pelletized P25 TiO_2 samples. The XRD spectra of both samples are shown in Fig. 4-3.

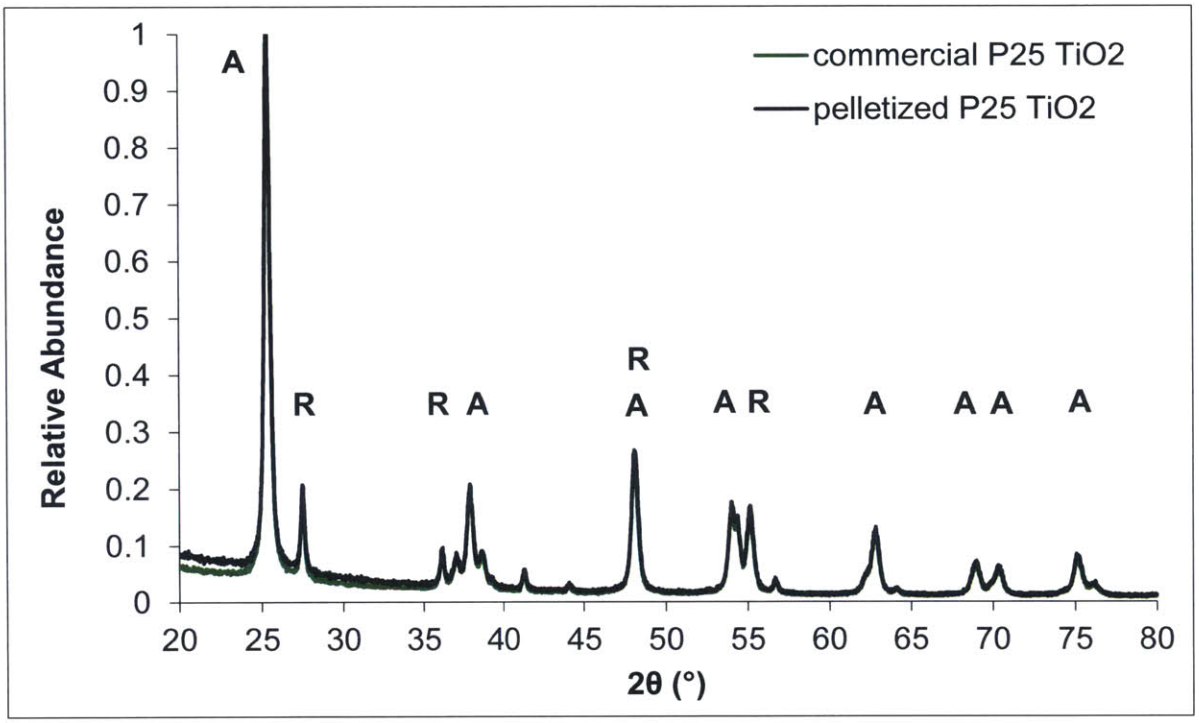

Figure 4-3. XRD spectra of commercial P25 TiO_2 nanopowder and pelletized P25 TiO_2 with marked anatase and rutile phases. Scan taken at 2°/min with Cu Kα source (λ = 0.1540 nm).

From this comparison it is clear that the method used to prepare the pelletized P25 TiO_2 had little to no effect on the material's crystallinity. This is consistent with what was found in the literature.[43] Peaks attributed to anatase (~75%) and rutile (~25%) are labeled as "A" and "R", respectively.

A low-temperature nitrogen adsorption-desorption experiment was carried out using a Quantachrome AutosorbiQ automated gas sorption analyzer, after degassing at 100 °C for 10 hours. The adsorption-desorption plots are shown below in Fig. 4-4. The BET method was used to calculate the surface area of the pelletized sample material, which was measured to be 57 m^2/g (commercial P25 TiO_2 nanopowder has BET surface area of 55 m^2/g).[36] This experiment

confirmed that the preparation method did not result in a decrease in surface area, which is usually a very important component of catalyst activity.

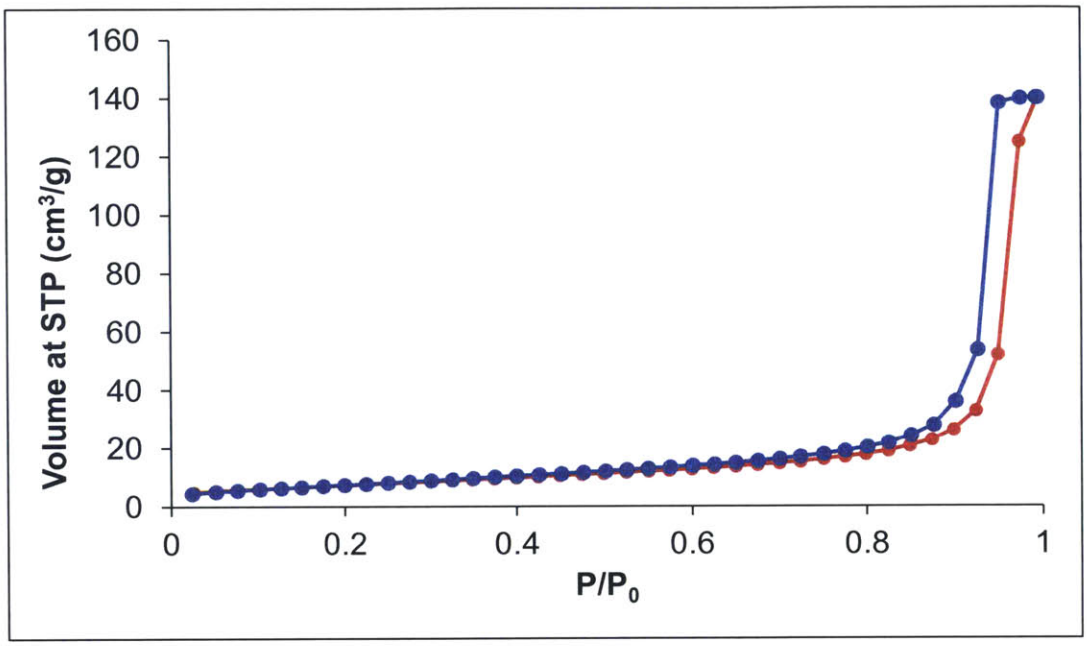

Figure 4-4. Low temperature (77 K) N_2 isotherms for adsorption (red)-desorption (blue) on pelletized P25 TiO_2.

The average pore size is 63 nm as calculated using the BJH method. This is consistent with the literature[43], which states that this material is macroporous. The total pore volume is 0.452 cm^3/g.

4.2.2 Activated hydrotalcite-like compound

As mentioned previously, the active sites in the acid-base aldol condensation over a HTlc are the OH-pairs. It is proposed[27] that it is the pairs on the basal surfaces that are the accessible active sites. The HTlc is activated through a series of steps to replace the carbonate anions in the interlayer galleries in hydrotalcite (HT), $Mg_6Al_2CO_3(OH)_{16} \cdot 4H_2O$, with these active hydroxyl groups. The end chemistry then should be $Mg_6Al_2(OH)_{18} \cdot 4H_2O$, with two hydroxyl groups

substituted for one carbonate group in the interlayers to maintain charge neutrality. This material is also known as meixnerite.

A commercial HT (Sigma Aldrich) was used as the starting material. HT was first calcined at 500 °C for 8 hours under N_2 flow. At this temperature, the HT undergoes a phase transition from the layered double hydroxide structure to an oxide. At 100 °C, physisorbed water is removed, followed by intercalated water molecules between 140 - 190 °C.[40,44] By 500 °C, the material has lost its interlayer anions and the brucite-like sheets have decomposed into an oxide of the parent metal, in this case Mg, with Al substitutions on the rock salt lattice.[40] XRD spectra comparing the calcined HT with MgO are shown in Fig. 4-5, using a Cu Kα source (λ = 0.1540 nm) taken at 2°/min. The spectrum of the calcined HT sample has peaks characteristic of a weakly crystalline MgO, namely reflections on the (111), (200), (220), (311), and (222) planes.[40,45] The significant peak broadening and associated loss of crystallinity is due to small (~5 nm) Mg-Al-O domains in the oxide.[40]

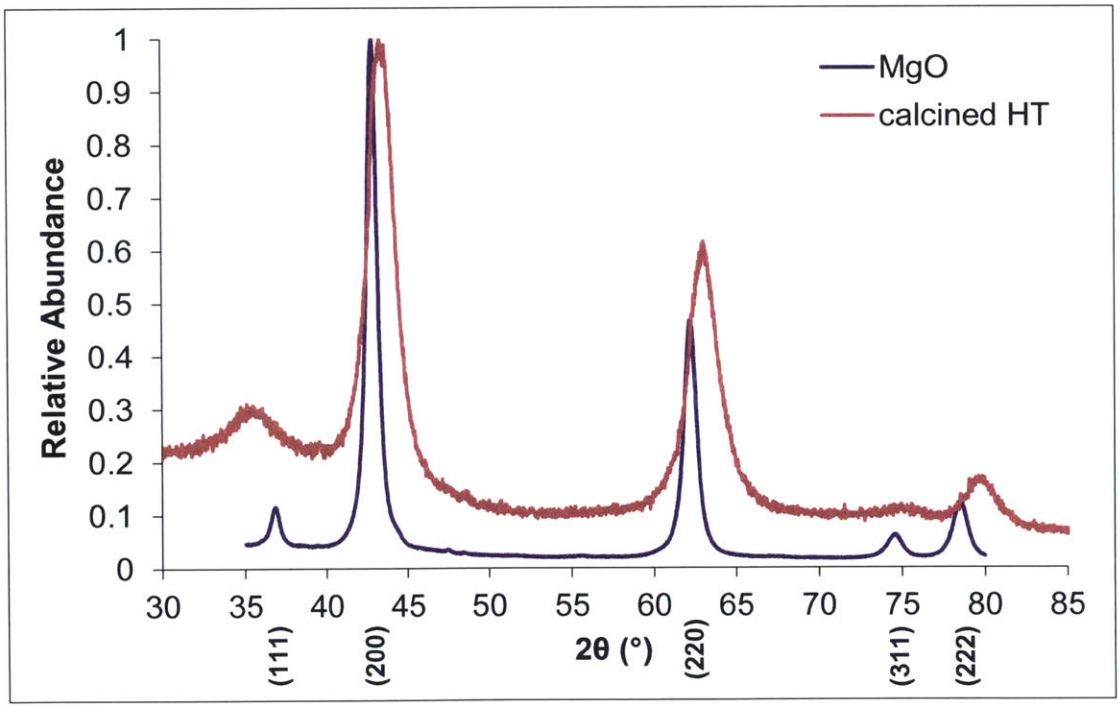

Figure 4-5. XRD spectra of calcined HT and MgO with crystal planes of MgO labeled.

The second step to activate the HT is to rehydrate the calcined HT to regenerate the layered double hydroxide phase with hydroxyl groups, the active sites in the condensation reaction, in place of the interlayer carbonate. First, water was decarbonated by bubbling N_2 into DI water for 3 hours in a sonicating bath to help remove dissolved CO_2. Next, the calcined HT was dispersed into the decarbonated water under N_2 flow for 5 hours at room temperature and intermittently stirred to aid in the rehydration process. After 5 hours the water was decanted and the sample was vacuum filtered to remove excess water. The material was then dried at 110 °C for 10 hours. The resulting sample will be identified as rehydrated HT.

After activating the HT, XRD was run on both samples to compare phases and to see if any changes could be noted due to the carbonate replacement with OH-. The similar XRD spectra as shown by Fig. 4-6 confirm that the layered double hydroxide structure was successfully regenerated upon rehydration of the oxide.

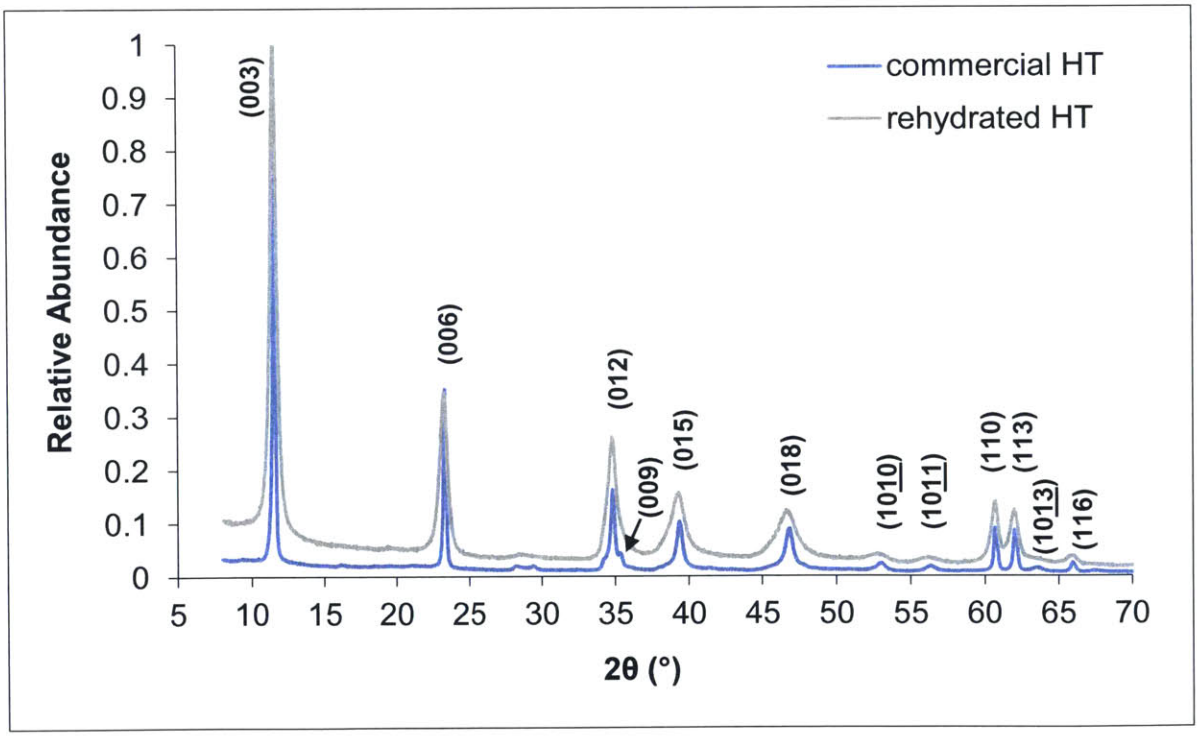

Figure 4-6. XRD spectra of commercial HT and rehydrated HT (meixnerite).

However, there was some loss of crystallinity during the calcination-rehydration process as shown by peak broadening especially on the (10$\underline{1}$0), (10$\underline{1}$1) and (10$\underline{1}$3) crystal planes.

In addition to phase identification, XRD is also useful in determining interplanar distance according to Bragg's Law (shown for n =1, for two neighboring unit cells):

$$sin\theta = \frac{\lambda}{2d},$$

where θ refers to the angle of diffraction, λ is the incident beam wavelength, and d is the normal distance between two lattice planes. XRD then can be used to investigate changes in basal plane spacing due to the replacement of carbonate groups by hydroxyl groups. This is the d-spacing as labeled in Fig. 4-7.

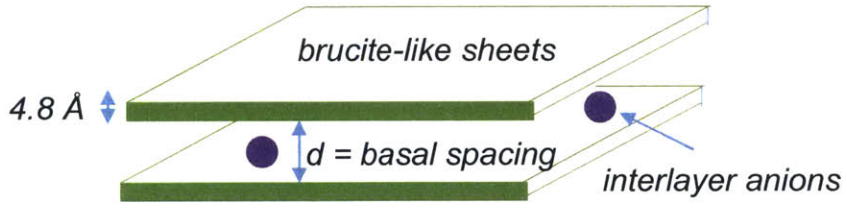

Figure 4-7. Basal plane spacing (d) varies with different interlayer anions in HTlc.

These changes are attributed more to the nature of the bonding between the anion and the brucite-like layers rather than to the size of the anion itself.[46] In the commercial and rehydrated HT materials the basal planes correspond to the (003), (006) and (009) peaks as labeled in Fig. 4-6. In the literature[27,38,40,46] the (003) plane is most commonly used for determining changes in interplane spacing due to the presence of different interlayer groups. The values for the basal plane spacing are listed in Table 4-2[38,40,46].

$d_{OH^-}^{003}$ (Å)	2.75
$d_{CO_3^{2-}}^{003}$ (Å)	2.85
2θ shift (°)	0.4

Table 4-2. D-spacing values between (003) planes for rehydrated hydrotalcite (interlayer hydroxyl) and commercial HT (interlayer carbonate). This relates to a 2θ shift in XRD spectra for the peaks corresponding to the (003) plane.

It is difficult to observe the relatively subtle 2θ shift of 0.4° given the resolution of the XRD spectra. As a result, another method was used to confirm that interlayer carbonate was successfully replaced by hydroxyl groups.

It is difficult to truly replace all of the CO_3^{2-} because invariably some CO_2 will enter the system either during hydration or drying.[47] To confirm that meixnerite was actually produced and hydrotalcite was not reformed during the rehydration process, x-ray photoelectron spectroscopy (XPS) was run on the samples to compare surface carbon content. The surface composition was assumed to approximately represent the bulk composition. As shown in Fig. 4-8, commercial HT has significantly more C in the first few atomic layers than rehydrated HT. The approximate mole composition comes out to 11 and 48% for rehydrated and commercial HT, respectively, confirming that rehydrated HT in the form of meixnerite was successfully produced.

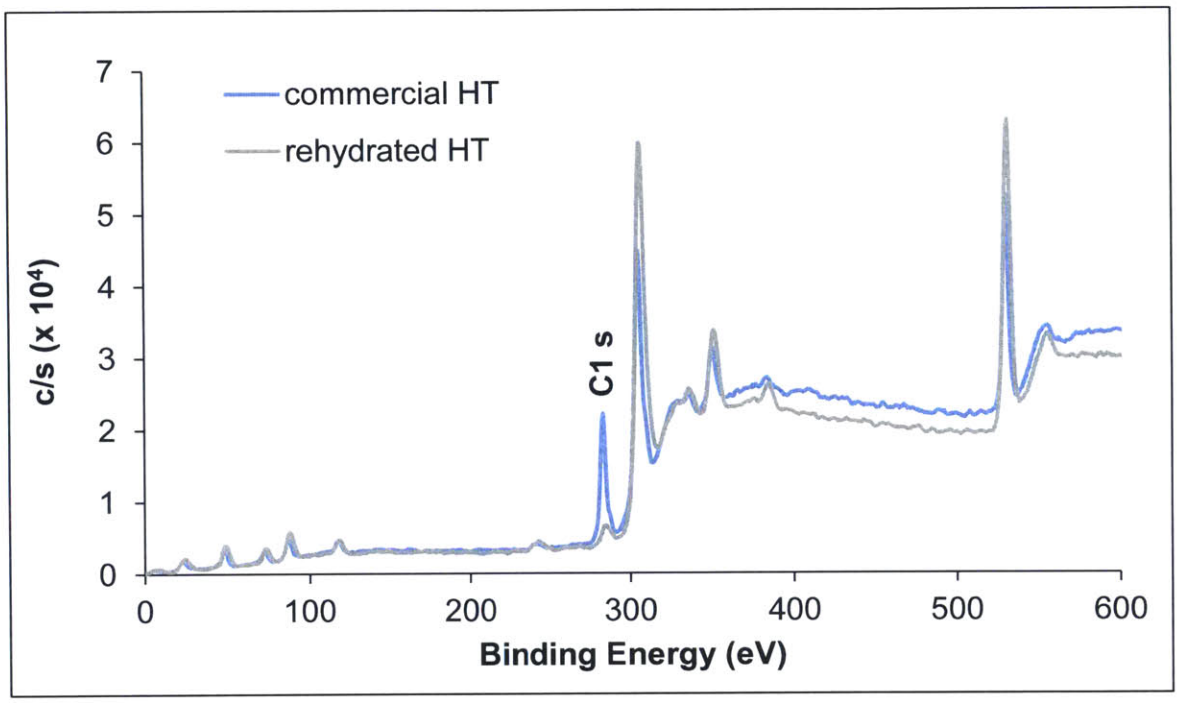

Figure 4-8. XPS spectra of commercial and rehydrated HT.

Similar to pelletized P25 TiO_2, a low-temperature nitrogen adsorption-desorption experiment was carried out after degassing at 80 °C for 8 hours. Isotherms for this experiment are shown in Fig. 4-9. The BET method was used to calculate the surface area of the rehydrated material, which was measured to be 21.3 m^2/g. This was lower than literature values, but this is not surprising as the authors[27] had control over surface areas through the synthesis methods (co-precipitation, urea decomposition), which was not the case for the commercial HT. Nevertheless, the differences in surface area need to be taken into account when comparing performance of the catalysts.

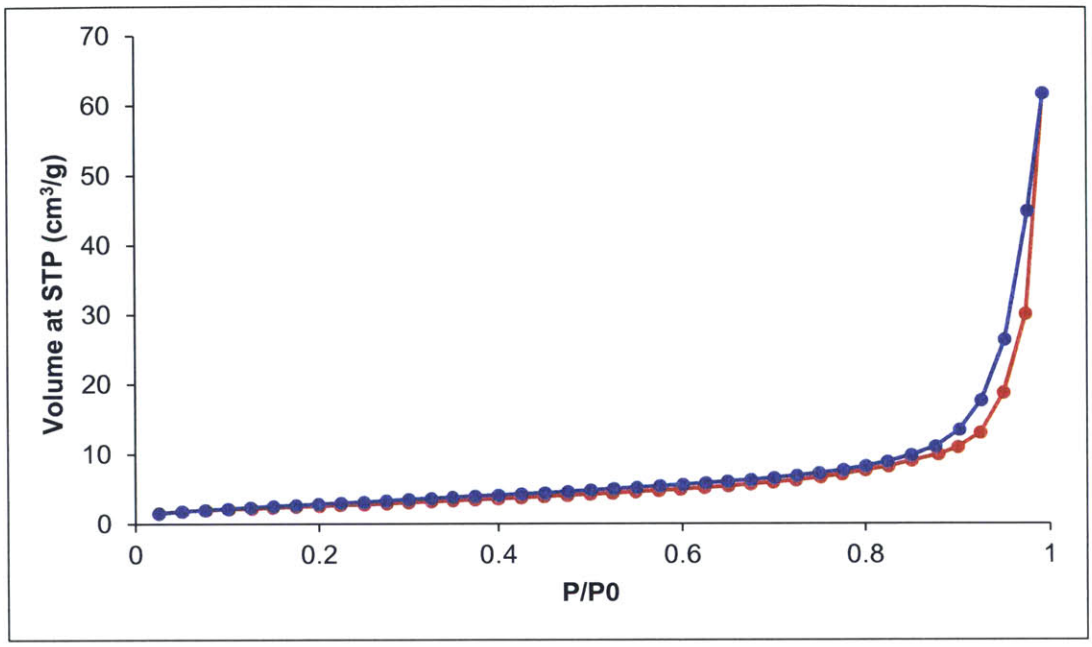

Figure 4-9. Low temperature (77 K) N_2 isotherms for adsorption (red)-desorption (blue) on rehydrated HT.

The BJH method was used to calculate average pore size and pore volume. The average pore size was 56 nm, suggesting a macroporous material. Total pore volume was measured to be 0.20 cm^3/g.

4.3 Thermal Stability

Many of the reactions that use P25 TiO_2 and HTlcs as catalysts are run at relatively mild temperatures. For example, photocatalytic oxidation of ethanol and aldol condensations often take place at room temperature, while some HTlc-catalyzed condensations are even run at 0 °C.[28] In this work, a traditional batch reaction is transitioning to a flow system, so it is possible that in order to get appreciable conversion, higher temperatures than the usual 0 to 80 °C are necessary. It was necessary then to evaluate the thermal stability of the pelletized P25 TiO_2 and rehydrated HT to establish the maximum reaction temperatures before either material decomposition or

phase transition occurs. To examine this, the samples were run in a thermogravimetric analyzer (TGA), and weight change as a function of temperature was measured. The derivative weight change versus temperature is plotted in Fig. 4-10.

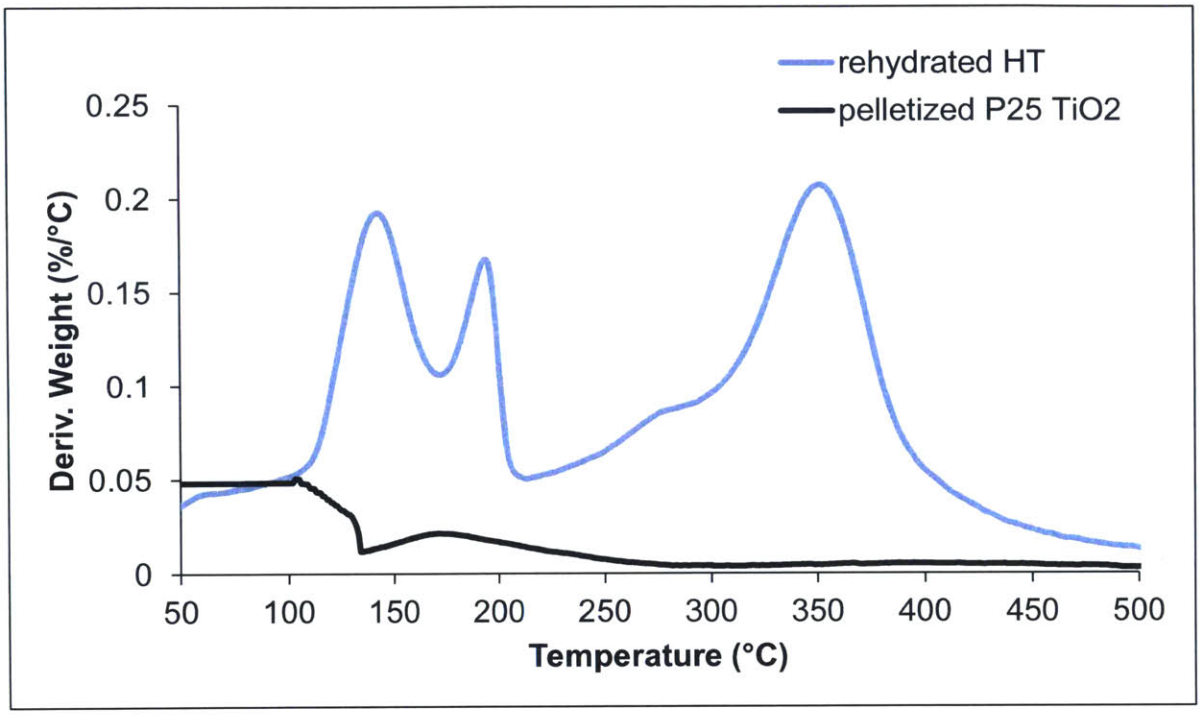

Figure 4-10. TGA of pelletized P25 TiO_2 and rehydrated HT samples.

There are two distinct peaks for the pelletized P25 TiO_2 sample that can both be attributed to the loss of molecularly adsorbed water. The first loss is likely due to any water that was not fully removed during the drying step in the preparation of the P25 TiO_2 pellets. The second is due to loss of surface hydration, which occurs as shown between 150 and 300 °C.[34] While not reflected in Fig. 4-10, hydroxyl groups interact to form water and desorb at 350 and 500 °C, resulting in dehydroxylation.[34] Even after outgassing at 200 °C, the P25 TiO_2 surface remains extensively hydroxylated.[36] Additionally, the phase transition from anatase to rutile occurs at temperatures greater than 700 °C. For pelletized P25 TiO_2 then, temperatures less than 350 °C maintain the active sites for this reaction.

Similar to pelletized P25 TiO_2, rehydrated HT experiences two weight losses between 100 and 200 °C related to the loss of molecular water. The first peak is attributed to dehydration of physisorbed water, while the second is due to loss of water in the interlayer galleries.[40] Between 140 and 160 °C, a metastable phase forms which represents the dehydrated HTlc, in which the layered double hydroxide structure is maintained but without water molecules intercalated between the brucite-like sheets. As the temperature is further increased there are two more distinct weight losses, which can be attributed to loss of interlayer anions (~275 °C) and the decomposition of the brucite-like layers. Another metastable phase forms between 240 and 260 °C, which corresponds to the layered double hydroxide phase without charge-compensating anions present.[44] The decomposition of the brucite-like layers at higher temperatures causes hydroxyl group loss in the form of H_2O and the phase transition into the weakly crystalline oxide, as shown previously by XRD of the calcined HT sample. With respect to the rehydrated HT as a catalyst, reaction temperatures below 250 °C safely avoid loss of active sites through dehydroxylation. Higher temperatures are of course possible, but the reaction mechanism will change as the weakly crystalline oxide that forms from the calcination of a HTlc behaves as a very basic catalyst.[30] Interlayer water molecules block access to accessible sites, so temperatures greater than 140-160 °C might help the reaction by increasing hydroxyl group access. This is the case for basal hydroxyl group active sites, but not for edge-only sites.[27,40]

Chapter 5

Performance of acid-base catalysts in acetaldehyde polycondensation in flow

5.1 Temperature experiments

The first set of tests was run at a fixed residence time over a range of temperatures from 50 to 200 °C over pelletized P25 TiO_2. The residence time was 2.5 minutes, which corresponds to the current minimum stable flowrate through the flow system (0.300 mL/min). A high residence time was chosen because initial experiments previously run in flow over a MgO catalyst did not show conversion until 300 °C at higher residence times. The bed was fully packed with the catalyst on a bed of quartz wool, amounting to 500 mg of pelletized P25 TiO_2 between 75 and 125 μm. No conversion was observed at 50 °C, but conversion increased to approximately 80% at 75 °C and 100% for both 150 and 200 °C, as shown in Fig. 5-1. While conversion was high at temperatures of 75 °C and greater, no products were observed in the liquid phase. GC parameters were adjusted to maximum inlet temperature and maximum oven temperature to ensure that any heavy condensation product would appear in the chromatograph.

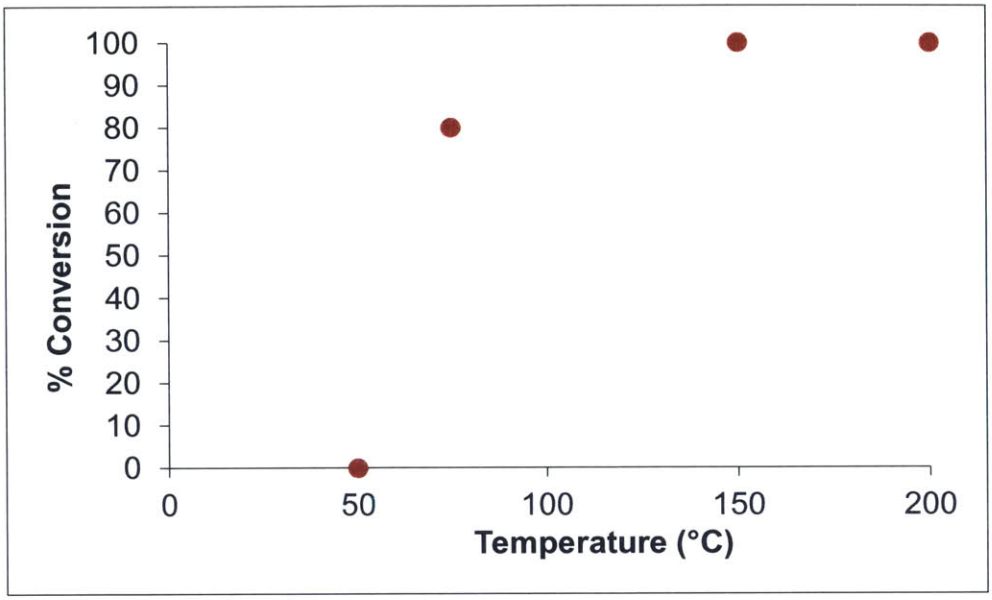

Figure 5-1. Conversion of acetaldehyde over a range of temperatures at fixed residence time (2.5 minutes) over pelletized P25 TiO_2.

The catalyst turned from white (fresh) to a deep orange, which is indicative of a polymer deposited on the surface. TGA was run on all spent catalysts, and is shown for those that came from the 150 °C and 200 °C runs in Fig. 5-2, compared to a baseline pelletized P25 TiO_2.

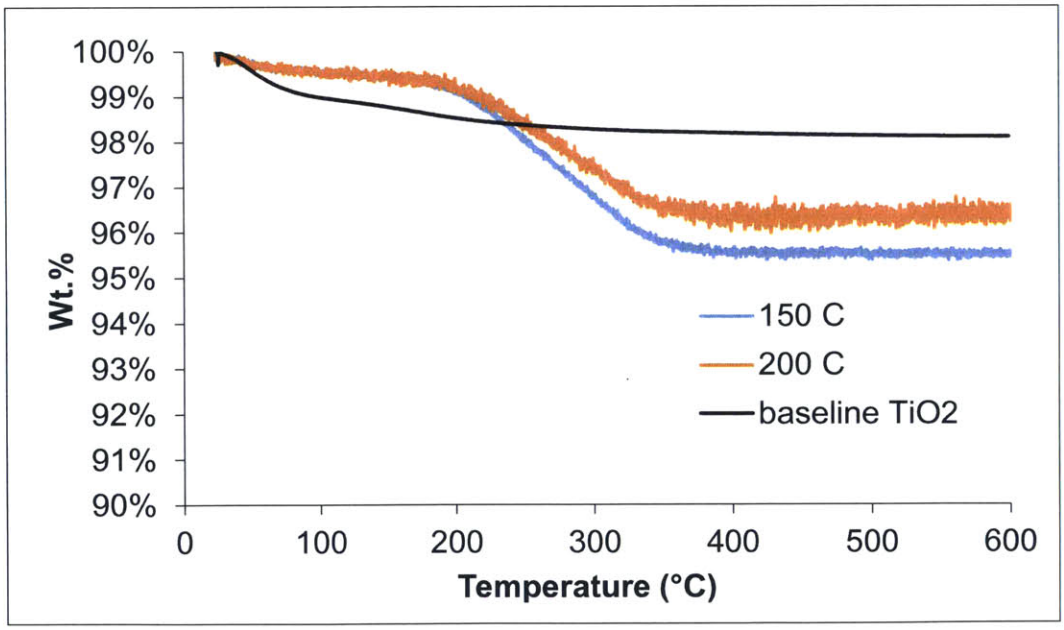

Figure 5-2. TGA of spent catalysts compared to fresh pelletized P25 TiO_2.

Between 200 and 400 °C there is a weight loss that can be attributed to the oxidation of carbonaceous compounds adsorbed on the surface. (The mass loss difference between the two samples is not quantitative because the catalysts were kept on stream for different amounts of time.) The spent catalyst was also sonicated in various solvents, including acetone, toluene, and dichloromethane, in an effort to desorb more loosely-bound compounds for evaluation through GC-MS. However, none of the adsorbates was removed through sonication. This is consistent with Luo and Falconer's finding[33] that even TPD and TPH at elevated temperatures could not sufficiently desorb condensates from the catalyst surface. The conversion of acetaldehyde resulted in high molecular weight condensation products, as expected. This preliminary set of tests showed that the reaction system will need tuning with respect to residence time, temperature, and the nature of the packed bed itself in order to gain better control of the reaction, with the goal to truncate the polycondensation to produce intermediates.

The temperature of the reaction is bound not only by catalyst stability but also by condensation product boiling point. Because the system is run in the gas phase, it is imperative that all reactants and products stay vaporized throughout the packed bed and up until the GC vial, where everything will condense in solution. Products that condense in the bed will yield a two-phase system in the reactor, causing two separate residence times for each phase. While the gas phase residence time could still be controlled, the liquid phase would essentially stay in the bed throughout the course of the reaction. The smallest condensation product, the dimer (crotonaldehyde), boils at 104 °C. Subsequently higher condensation products boil at higher temperatures, as shown in Table 5-1. To obtain an intermediate condensation product of interest, the temperature in the bed during reaction has to be at least the boiling point temperature.

Salicylaldehyde ($C_7H_6O_2$), syringaldehyde ($C_9H_{10}O_4$), and cuminaldehyde ($C_{10}H_{12}O$) are used as example higher condensation products with a cyclized chemistry.

#C	Compound	Boiling Point (°C)
2	Acetaldehyde	21
4	Crotonaldehyde	104
6	Sorbaldehyde	173
7	Salicylaldehyde	196
9	Syringaldehyde	192
10	Cuminaldehyde	235

Table 5-1. Boiling points of condensation products of acetaldehyde, along with potential higher order condensation products with cyclized chemistries.

From here, 200 °C can be taken as the minimum reaction temperature because (1), 100% conversion was already observed at this temperature, and (2), several condensation products of interest are comfortably in the gas phase at this temperature.

5.2 Residence time experiments

Experiments were run with both pelletized P25 TiO_2 and rehydrated HT catalysts at a fixed temperature of 200 °C over a range of residence times. Flowrates of acetaldehyde are summarized in Table 5-2, and results from these reaction conditions are shown in Fig. 5-3.

	Acetaldehyde Flowrate	
Residence Time (min)	*(μmol/min)*	*(mL/min)*
2.5	9	0.22
1.5	13	0.33
1	23	0.57
0.5	34	0.85

Table 5-2. Acetaldehyde flowrates for different residence times.

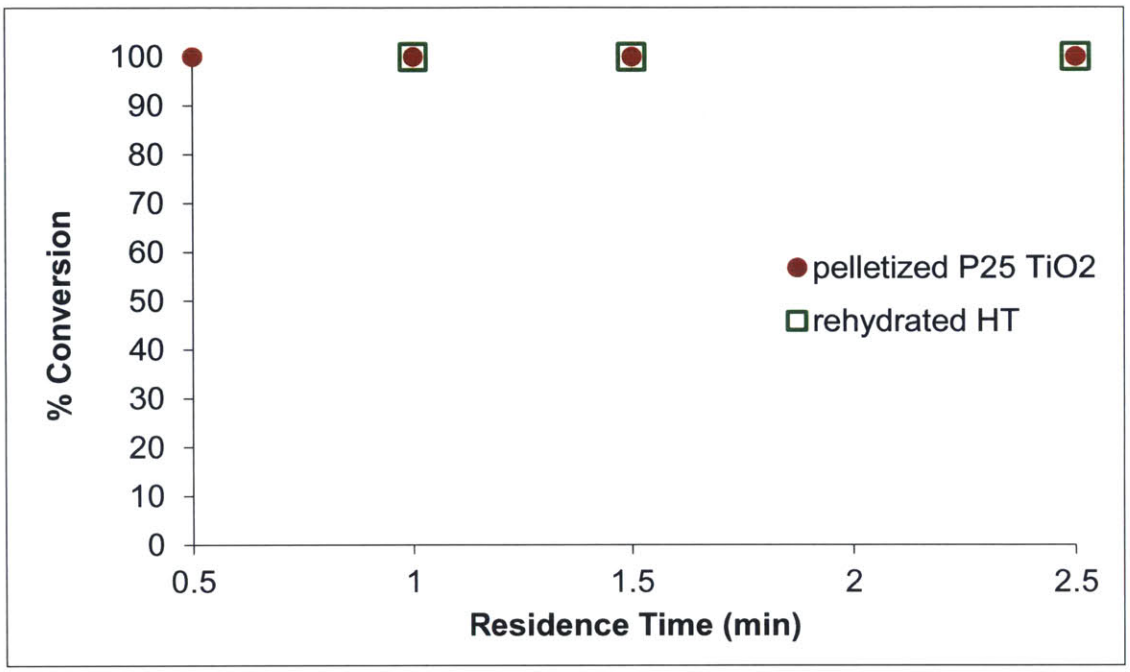

Figure 5-3. Conversion of acetaldehyde at 200 °C over residence times from 0.5 to 2.5 minutes.

Approximately 500 mg of pelletized P25 TiO_2 and 350 mg of rehydrated HT, sized between 75 and 125 μm, were used in the full packed bed volume. At all residence times over both catalysts, conversion was 100%. Even at relatively short residence times (30 seconds to 1 minute), no liquid phase products were observed. Over pelletized P25 TiO_2, a similar deep orange was observed on the spent catalyst. Significant deposition was also observed on the spent rehydrated HT catalyst as shades of gray. This color is suggestive of coke deposition rather than polymerization. It is not surprising that the resultant heavy condensation products have different chemistries because the active sites behave differently in terms of Lewis-Bronsted nature as well as site strength. The spent catalysts are shown in Fig. 5-4.

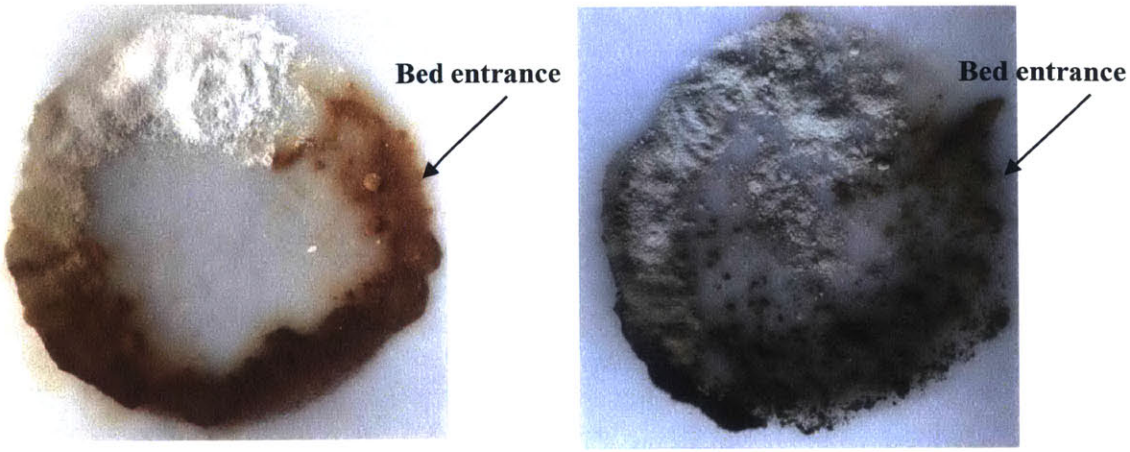

Figure 5-4. Spent catalysts after reactions at 200 °C in the full packed bed.

It is interesting to note that the catalyst color changes along the length of the reactor bed. The beginning of the bed adsorbed the most acetaldehyde and subsequently less was adsorbed with increasing depth into the reactor (clockwise in Fig. 5-4). The catalyst at the end of the reactor maintained the color of the fresh catalyst (white and light brown for pelletized P25 TiO_2 and rehydrated HT, respectively). This can be attributed to decreasing concentrations of acetaldehyde in the vapor phase as it passes through the reactor. The maximum concentration (the flowrates outlined in Table 5-2) enters the bed, and a fraction of the acetaldehyde adsorbs in the first regime, reducing the concentration in the stream that proceeds to the next bed regime. A fraction of this will adsorb as well, but because the vapor is less concentrated in this stage the amount is reduced. This trend proceeds until there is no acetaldehyde left in the vapor phase, as shown by the uncolored final regime of the catalyst bed. Conversion is 100% before the end of the bed is reached.

5.3 Shortened bed experiments

This motivated looking into what components of the reaction are actually responsible for the conversion. The three main causes are temperature, physical adsorbance, and active sites. To test this, controls were run with blank beds at a fixed residence time of 30 s over a range of temperatures, as well as with the commercial (inactive) HT, as shown in Fig. 5-5.

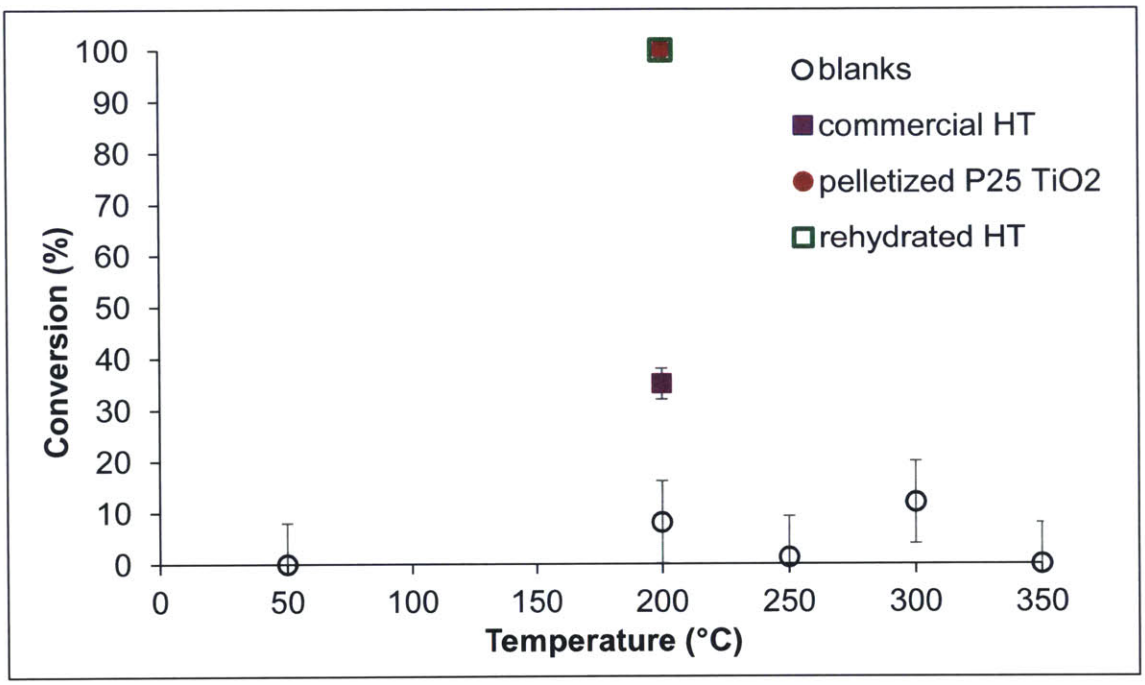

Figure 5-5. Acetaldehyde conversion with a 30 s residence time in various packed bed conditions.

From temperatures of 50 to 350 °C, between 10 to 15% conversion can be attributed just to temperature. It is not surprising that the acetaldehyde reacts at higher temperatures even in the absence of a catalyst, because it is a very reactive compound that has been shown to even polymerize to paraldehyde at room and sub-room temperatures.[48] The next control was to ensure that the active sites, rather than just physical adsorbance, were responsible for most of the conversion of the acetaldehyde. Otherwise, tuning catalyst activity and the nature of the active sites themselves would be irrelevant. The control used a full packed bed (approximately 350 mg)

of commercial HT, which has been shown to be inactive in the literature[25,27] because it does not possess the active hydroxyl groups in the interlayer galleries. Conversion over this material was 35 ± 2% at 200 °C, and at the same condition for the blank was 8 ± 8%. From this, it can be concluded that at these conditions anywhere from 17 to 37% of conversion is due physical adsorbance—the acetaldehyde polymerizes simply because it has something on which to adsorb and further react with itself. That leaves between 63 and 83% of conversion due to the active sites of the catalyst. This confirms that the reaction can be significantly controlled by the catalyst itself. These control studies motivated the shortening of the catalyst bed in an effort to reduce conversion by physical adsorption alone, which results in solids deposition on the catalyst surface. A schematic of the shortened bed is shown in Fig. 5-6.

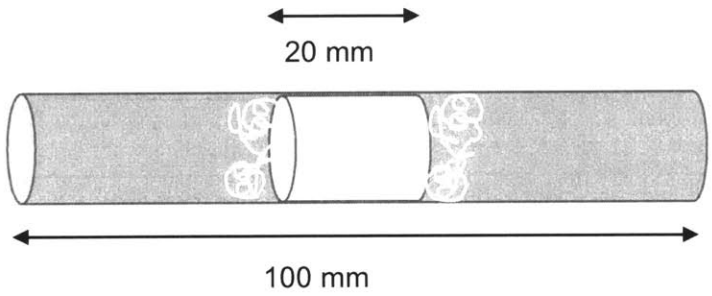

Figure 5-6. 100 mm packed bed reactor partially packed (20%) to reduce conversion due to physical adsorbance.

The catalyst bed was shortened from 100 mm down to 20 mm, using 20% of the full packed bed mass. Reducing the length of the catalyst bed has two effects: decrease in vapor-solid contact, and reduction in the full packed bed's minimum residence time. The shortened bed cut the original minimum residence time by an order of magnitude, from 10 seconds down to 1 second. This allows for a wider range of parameter space to test and provides further control over the polycondensation reaction. In these experiments, the same tube reactor and heating system were used. Experiments were run with approximately 100 mg of pelletized P25 TiO_2 and 70 mg

of rehydrated HT in the same average particle size range (75-125 μm), to keep residence times fixed between the two catalysts. Quartz wool was used to keep the catalyst in the center of the bed, as shown in Fig. 5-6.

All tests were run at 200 °C at mass flow controller setpoints of 1.000, 3.000, and 4.000 mL/min. These flows correspond to 6.6, 2.4, and 1.5 s residence times, respectively. The results are shown in Fig. 5-7. Over pelletized P25 TiO_2, conversion dropped by approximately 10% across all residence times compared to the same conditions over the full packed bed. Similarly, conversion dropped between 10-25% over rehydrated HT. The trend appears to be an increase in conversion with decrease in residence time. However, the increase is within fluctuations of the system and thus, conversion can be taken as approximately constant for the reactions over both catalysts at all residence times. A control using commercial HT was run at 6.6 residence time using the 20% packed bed configuration for support that these reductions in conversion were due to reductions in conversion by physical adsorbance. The conversion over the control decreased by approximately 10% from the full to 20% packed bed, which is consistent with the other samples. This confirms that this configuration reduces selectivity towards acetaldehyde deposition on the catalyst surface.

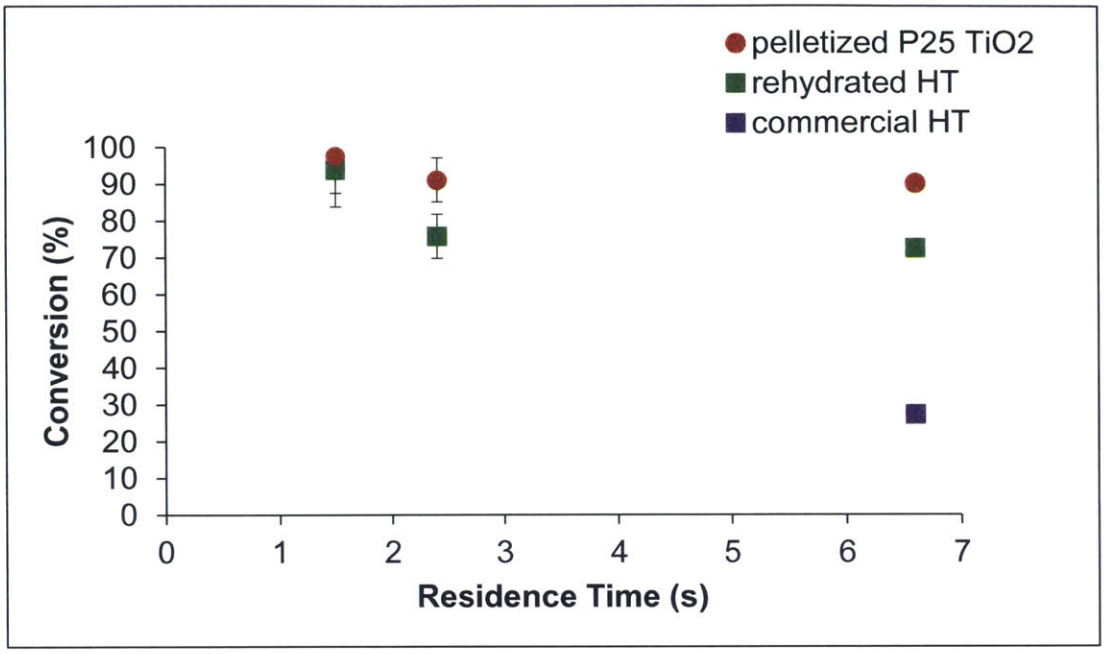

Figure 5-7. Conversion of acetaldehyde at a fixed temperature (200 °C) over a range of residence times in the 20% packed bed configuration.

A further promising result arose from the shortened bed experiments as well. Unlike in previous reactions over the full packed bed, the 20% configuration produced a liquid phase condensation product. The dimer of acetaldehyde, crotonaldehyde, was observed through GC-MS, as shown in Fig. 5-8. Additionally, small amounts of butanal (unsaturated crotonaldehyde), were observed as well. By simply shortening the bed, selectivity towards liquid phase condensation products increased due to the decrease in conversion by adsorption alone. This is consistent with the color homogeneity and reduced color intensity of the spent catalysts. While yields were low and the dimer is outside of the desired chemistry range for fuel-size molecules, it is exciting that selectivity towards liquid phase products increased and yields were observed on the order of seconds for a typically batch-run reaction. The reaction conditions need to be further optimized to increase liquid phase yields and selectivity towards intermediate compounds.

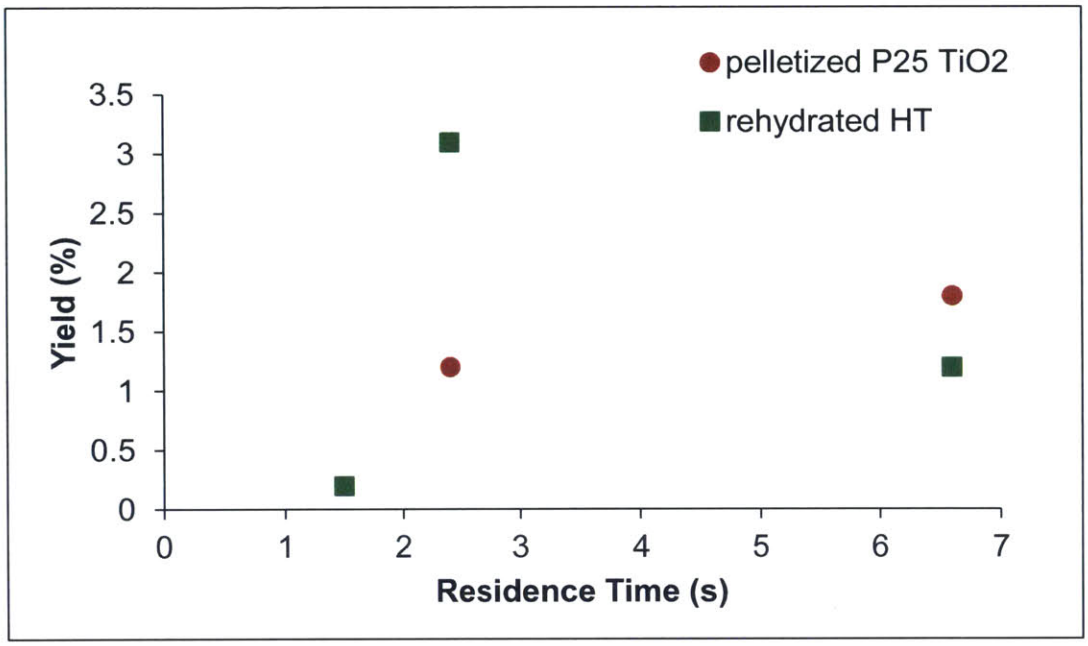

Figure 5-8. Yields of the dimer of acetaldehyde condensation, crotonaldehyde, in the 20% packed bed configuration at 200 °C. Yields at 1.5 s overlap for both catalyst samples.

As a trial experiment, the same 20% packed bed configuration was run but without preheating of the acetaldehyde vapor. The same bed was used and partially packed, but heating tape was used to heat only the catalyst bed rather than the chuck-cartridge heating system that heats the entire 100 mm. At the same residence time of 2.4 s and temperature of 200 °C, in the absence of reactant preheating yields of the dimer increased to 5% over the pelletized P25 TiO_2 catalyst. The rehydrated HT yields did not increase. Clearly further adjustment of the system parameters is required, but with the wide range of temperatures and residence times afforded by this system, as well as the flexibility in the nature of the packed bed itself, more control over the polycondensation and higher selectivity are possible. Future work can investigate more of the temperature space; catalyst active sites in terms of number, strength, and acid-base character; and means of polycondensation suppression including competitive adsorption and chemical inhibition.

Chapter 6

Conclusion

Generating transportation fuels from carbon-neutral sources like bio-oil is desired to help retard the increasing levels of atmospheric carbon dioxide and the associated climate change effects. The chemistry and reactivity of acetaldehyde make it a very representative model compound for bio-oil, and thus was investigated in this work in a controlled polycondensation reaction. A polycondensation reaction is of interest because single aldol condensations of such bio-oil model compounds yield products with insufficient energy densities and limited physical properties required for transportation fuels. Pelletized Evonik P25 TiO_2 and an activated HTlc were chosen for evaluation as catalysts in this reaction because they possess the acid-base sites suggested to be active in promoting a polycondensation reaction. To evaluate these materials, a flow system was developed that mimics the conditions of a theoretical process step in the overall bio-oil upgrading scheme. The system targets pyrolysis vapors as they are quenched in the pyrolysis unit to help increase bio-oil stability and address the challenges associated with its transportation, storage, and processing. The flow system is flexible in that many different temperatures, residence times, and packed bed parameters can be easily adjusted.

The catalyst materials were prepared and characterized with XRD, low-temperature N_2 adsorption-desorption experiments, XPS, and TGA. The HTlc was successfully activated

through a calcination-rehydration process, generating the acid-base hydroxyl pairs that promote the condensation reaction. The catalysts were proven to be active in the polycondensation of acetaldehyde, achieving high conversion despite the transition from typical batch conditions to flow. Selectivity to deposition on the catalyst was high, but by shortening the length of the packed bed and decreasing the residence time liquid phase products were formed on the order of seconds. Further tuning of the reaction system, including optimal reaction temperatures, residence times, and catalyst activity, has the potential to significantly increase selectivity to intermediate condensation products, providing a feasible pathway for supplementing petroleum-derived fuels with a carbon-neutral alternative.

Bibliography

(1) U.S. Energy Information Administration http://www.eia.gov/cfapps/ipdbproject/iedindex3.cfm?tid=90&pid=44&aid=8 (accessed Apr 25, 2015).

(2) Fabricius, K. E.; Langdon, C.; Uthicke, S.; Humphrey, C.; Noonan, S.; De'ath, G.; Okazaki, R.; Muehllehner, N.; Glas, M. S.; Lough, J. M. Losers and Winners in Coral Reefs Acclimatized to Elevated Carbon Dioxide Concentrations. *Nat. Clim. Chang.* **2011**, *1* (3), 165–169.

(3) Fricker, K. J.; Park, A. H. A. Effect of H_2O on $Mg(OH)_2$ Carbonation Pathways for Combined CO_2 Capture and Storage. *Chem. Eng. Sci.* **2013**, *100*, 332–341.

(4) Farrauto, R. J.; Duyar, M. S.; Arellano, M. Dual Function Materials for CO_2 Capture and Conversion using Renewable H_2. *Appl. Catal. B Environ.* **2015**, *168*, 370–376.

(5) EPA Climate Change http://www.epa.gov/climatechange/ghgemissions/sources/transportation.html (accessed Jan 1, 2015).

(6) Kahn Ribeiro, S.; Kobayashi, S.; Beuthe, M.; Gasca, J.; Greene, D.; Lee, D. S.; Muromachi, Y.; Newton, P. J.; Plotkin, S.; Sperling, D.; et al. Transport and its Infrastructure. In *Climate Change 2007: Mitigation*; Bose, R., Kheshgi, H., Eds.; Cambridge University Press: Cambridge, United Kingdom; New York, New York, USA, 2007; pp 323–385.

(7) Adjaye, J. D.; Bakhshi, N. N. Production of Hydrocarbons by Catalytic Upgrading of a Fast Pyrolysis Bio-oil. Part II: Comparative Catalyst Performance and Reaction Pathways. *Fuel Process. Technol.* **1995**, *45* (3), 185–202.

(8) Wang, M.; Han, J.; Dunn, J. B.; Cai, H.; Elgowainy, A. Well-to-Wheels Energy Use and Greenhouse Gas Emissions of Ethanol from Corn, Sugarcane and Cellulosic Biomass for US Use. *Environ. Res. Lett.* **2012**, *7* (4), 1–13.

(9) IRENA. *Production of Liquid Biofuels: Technology Brief*; 2013.

(10) Guo, M.; Song, W.; Buhain, J. Bioenergy and Biofuels: History, Status, and Perspective. *Renew. Sustain. Energy Rev.* **2015**, *42* (2015), 712–725.

(11) United States Department of Energy. *Replacing the Whole Barrel*; 2013.

(12) Huber, G. W.; Iborra, S.; Corma, A. Synthesis of Transportation Fuels from Biomass: Chemistry, Catalysts, and Engineering. *Chem. Rev.* **2006**, *106* (9), 4044–4098.

(13) Oasmaa, A.; Elliott, D. C.; Korhonen, J. Acidity of Biomass Fast Pyrolysis Bio-oils. *Energy and Fuels* **2010**, *24* (12), 6548–6554.

(14) Hoang, T. Q.; Zhu, X.; Sooknoi, T.; Resasco, D. E.; Mallinson, R. G. A Comparison of the Reactivities of Propanal and Propylene on HZSM-5. *J. Catal.* **2010**, *271* (2), 201–208.

(15) Diebold, J. P. *A Review of the Chemical and Physical Mechanisms of the Storage Stability of Fast Pyrolysis Bio-Oils*; 2000.

(16) Ivanova, L. V.; Koshelev, V. N.; Burov, E. A. Influence of the Hydrocarbon Composition of Diesel Fuels on their Performance Characteristics. *Pet. Chem.* **2014**, *54* (6), 466–472.

(17) Li, C. J. Organic Reactions in Aqueous Media with a Focus on Carbon-Carbon Bond Formations: A Decade Update. *Chem. Rev.* **2005**, *105* (8), 3095–3165.

(18) Zhao, C.; He, J.; Lemonidou, A.; Li, X.; Lercher, J. Aqueous-Phase Hydrodeoxygenation of Bio-derived Phenols to Cycloalkanes. *J. Catal.* **2011**, *280* (1), 8–16.

(19) Di Cosimo, J. I.; Díez, V. K.; Apesteguía, C. R. Base Catalysis for the Synthesis of α,β-Unsaturated Ketones from the Vapor-Phase Aldol Condensation of Acetone. *Appl. Catal. A Gen.* **1996**, *137* (1), 149–166.

(20) Snell, R. W.; Combs, E.; Shanks, B. H. Aldol Condensations using Bio-oil Model Compounds: The Role of Acid-Base Bi-functionality. *Top. Catal.* **2010**, *53* (15-18), 1248–1253.

(21) Díez, V. K.; Apesteguía, C. R.; Di Cosimo, J. I. Effect of the Acid-Base Properties of Mg-Al Mixed Oxides on the Catalyst Deactivation during Aldol Condensation Reactions. *Lat. Am. Appl. Res.* **2003**, *33* (2), 79–86.

(22) Zeidan, R. K.; Davis, M. E. The Effect of Acid-Base Pairing on Catalysis: An Efficient Acid-Base Functionalized Catalyst for Aldol Condensation. *J. Catal.* **2007**, *247* (2), 379–382.

(23) Di Cosimo, J. I.; Díez, V. K.; Ferretti, C.; Apesteguía, C. R. Basic Catalysis on MgO: Generation, Characterization and Catalytic Properties of Active Sites. **2014**, *26* (3000), 1–28.

(24) Gangadharan, A.; Shen, M.; Sooknoi, T.; Resasco, D. E.; Mallinson, R. G. Condensation Reactions of Propanal over $Ce_xZr_{1-x}O_2$ Mixed Oxide Catalysts. *Appl. Catal. A Gen.* **2010**, *385*, 80–91.

(25) Roelofs, J. C.; Lensveld, D. J.; van Dillen, A. J.; de Jong, K. P. On the Structure of Activated Hydrotalcites as Solid Base Catalysts for Liquid-Phase Aldol Condensation. *J. Catal.* **2001**, *203* (1), 184–191.

(26) Ordomsky, V. V.; Sushkevich, V. L.; Ivanova, I. I. Study of Acetaldehyde Condensation Chemistry over Magnesia and Zirconia Supported on Silica. *J. Mol. Catal. A Chem.* **2010**, *333*, 85–93.

(27) Lei, X.; Zhang, F.; Yang, L.; Guo, X.; Tian, Y.; Fu, S.; Li, F.; Evans, D. G.; Duan, X. Highly Crystalline Activated Layered Double Hydroxides as Solid Acid-Base Catalysts. *AIChE J.* **2007**, *53* (4), 932–940.

(28) Prinetto, F.; Ghiotti, G.; Giuria, V. P.; Durand, R.; Tichit, D. Investigation of Acid-Base Properties of Catalysts Obtained from Layered Double Hydroxides. *J. Phys. Chem. B* **2000**, *104*, 11117–11126.

(29) Climent, M. J.; Corma, A.; Fornés, V.; Guil-Lopez, R.; Iborra, S. Aldol Condensations on Solid Catalysts: A Cooperative Effect between Weak Acid and Base Sites. *Adv. Synth. Catal.* **2002**, *344* (10), 1090–1096.

(30) Dumitriu, E.; Hulea, V.; Chelaru, C.; Catrinescu, C.; Tichit, D.; Durand, R. Influence of the Acid–Base Properties of Solid Catalysts Derived from Hydrotalcite-like Compounds on the Condensation of Formaldehyde and Acetaldehyde. *Appl. Catal. A Gen.* **1999**, *178* (2), 145–157.

(31) Garrone, E.; Bartalini, D.; Coluccia, S.; Martra, G.; Tichit, D.; Figueras, F. UV-Vis Study of the Condensation Reaction of Carbonylic Compounds on MgO and Hydrotalcites. *Acid-Base Catal. II* **1994**, *90*, 183–193.

(32) Lippert, S.; Baumann, W.; Thomke, K. Secondary Reactions of the Base-catalyzed Aldol Condensation of Acetone. *J. Mol. Catal.* **1991**, *69*, 199–214.

(33) Luo, S.; Falconer, J. L. Acetone and Acetaldehyde Oligomerization on TiO_2 Surfaces. *J. Catal.* **1999**, *185* (2), 393–407.

(34) Bickley, R. I.; Gonzalez-Carreno, T.; Lees, J. S.; Palmisano, L.; Tilley, R. J. D. A Structural Investigation of Titanium Dioxide Photocatalysts. *J. Solid State Chem.* **1991**, *92* (1), 178–190.

(35) Martra, G. Lewis Acid and Base Sites at the Surface of Microcrystalline TiO_2 Anatase: Relationships between Surface Morphology and Chemical Behaviour. *Appl. Catal. A Gen.* **2000**, *200*, 275–285.

(36) Deiana, C.; Fois, E.; Coluccia, S.; Martra, G. Surface Structure of TiO_2 P25 Nanoparticles : IR Study of Hydroxy Groups on Coordinative Defect Sites. *J. Phys. Chem. C* **2010**, *114*, 21531–21538.

(37) Singh, M.; Zhou, N.; Paul, D. K.; Klabunde, K. J. IR Spectral Evidence of Aldol Condensation: Acetaldehyde Adsorption over TiO_2 Surface. *J. Catal.* **2008**, *260* (2), 371–379.

(38) Miyata, S. Anion-Exchange Properties of Hydrotalcite-like Compounds. *Clays Clay Miner.* **1983**, *31* (4), 305–311.

(39) Tronto, J.; Bordonal, A. C.; Naal, Z.; Barros Valim, J. Conducting Polymers / Layered Double Hydroxides Intercalated Nanocomposites. In *Materials Science - Advanced Topics*; Mastai, Y., Ed.; InTech, 2013; pp 3–31.

(40) Roelofs, J. C. A. A.; van Bokhoven, J. A.; van Dillen, A. J.; Geus, J. W.; de Jong, K. P. The Thermal Decomposition of Mg-Al Hydrotalcites: Effect of Interlayer Anions and Characteristics of the Final Structure. *Chem. A Eur. J.* **2002**, *8* (24), 5571–5579.

(41) Rao, K. Activation of Mg–Al Hydrotalcite Catalysts for Aldol Condensation Reactions. *J. Catal.* **1998**, *173* (1), 115–121.

(42) Ringer, M.; Putsche, V.; Scahill, J. *Large-Scale Pyrolysis Oil Production: A Technology Assessment and Economic Analysis*; 2006.

(43) Lillo-Ródenas, M. A.; Bouazza, N.; Berenguer-Murcia, A.; Linares-Salinas, J. J.; Soto, P.; Linares-Solano, A. Photocatalytic Oxidation of Propene at Low Concentration. *Appl. Catal. B Environ.* **2007**, *71*, 298–309.

(44) Stanimirova, T. S.; Vergilov, I.; Kirov, G. Thermal Decomposition Products of Hydrotalcite-like Compounds: Low-Temperature Metaphases. **1999**, *4*, 4153–4161.

(45) Dercz, G.; Prusik, K.; Pajak, L.; Pielaszek, R.; Malinowski, J. J.; Pudlo, W. Structure Studies on Nanocrystalline Powder of MgO Xerogel Prepared by the Sol-gel Method. *Mater. Sci. Pol.* **2009**, *27* (1), 201–207.

(46) Cavani, F.; Trifiro, F.; Vaccari, A. Hydrotalcite-Type Anionic Clays: Preparation, Properties and Applications. *Catal. Today* **1991**, *11*, 173–301.

(47) Delidovich, I.; Palkovits, R. Catalytic Activity and Stability of Hydrophobic Mg–Al Hydrotalcites in the Continuous Aqueous-Phase Isomerization of Glucose into Fructose. *Catal. Sci. Technol.* **2014**, *4*, 4322–4329.

(48) Bevington, J. C.; Norrish, R. G. W. The Polymerization of Acetaldehyde at Low Temperatures. *Proc. R. Soc. London, Ser. A* **1949**, *196* (1046), 363–378.